Eidgenössische Technische Hochschule Zürich
Swiss Federal Institute of Technology Zurich

Department of Information Technology
and Electrical Engineering

Benjamin Weber

Simulation Tool for Next Generation Cellular Networks

Semester Project Autumn Semester 2010

Departement:
D-ITET – Electrical Engineering, ETH Zurich

Tutor:
Raphael Rolny, Communication Technology Laboratory

Zurich, January 7, 2011

Picture on title page: Base station antennas in Mexico.

Abstract

In a research lab for cellular networks, simulating network topologies is a crucial part of exploring interesting layouts and promising communication techniques. Unfortunately, readying a simulation and analyzing the results can be a time consuming effort. In this work, a generic and modularly built simulation environment is presented. It can be used to simulate arbitrary network setups and, what's more, it can be enhanced easily to incorporate additional communication techniques. This tool is used to simulate a small selection of cellular networks. The comparison of conventional system and cooperation as well as relaying techniques are in focus.

Preface

This semester project is part of the Master program in Electrical Engineering and Information Technology at ETH in Zurich. It is mandatory to complete two semester projects.

The author certifies that this work was created by himself. This includes text, figures, and Matlab code. All third party material, which was copied, cited or reproduced in this report, has been referenced or acknowledged in an adequate form. Benjamin Weber

Contents

List of Figures

Chapter 1

Introduction

1.1 Motivation

Cellular networks have been existent for several decades. The demand for cellular coverage in urban areas as well as rural or slightly inhabited regions, has been constantly increasing. GSM, as the first purely digital cellular network standard, meets the requirements of a 2G network. Globally, it is the most widely deployed cellular standard. Roughly ten years later, the UMTS standard was able to cope with the 3G requirements. And soon, the first 4G networks will be deployed. This successive development is partly characterized by a constant increase of data rates in these networks. A 4G network should be able to provide up to 1 Gb/s peak data rate on the downlink. [7]

In order to understand and deploy a future cellular network, extensive research is necessary. Multiple-input multiple-output (MIMO) can be exploited more extensively. Promising techniques such as base station (BS) cooperation, relaying, multi-user MIMO, and coordinated multi-point transmission need to be analyzed. Unfortunately, up to the present, rate computations for an arbitrary cellular network can be highly complex. Simulation is an adequate remedy to understand the behavior of cellular networks. Nevertheless, let alone the preparation of a simulation, the realization of such an endeavor can be very time consuming.

A generic simulation environment with modularly built components is able to lessen simulation effort and give faster analysis of a given network. In this project, such a simulation tool is developed and used to simulate a small selection of cellular networks. Conventional networks shall be compared with BS cooperation and relaying.

1.2 Outline

This report is divided into the following chapters:

Chapter 2 gives a theoretic overview of the wireless channel and MIMO techniques. Aspects of a wireless environment are presented and characteristics, such as channel capacity, are discussed.

Chapter 3 describes briefly a few theoretic concepts of cellular networks. A network model is given and attributes, which are new in next generation cellular networks, are presented.

Chapter 4 presents the simulation environment developed as part of this work. A conceptual layout of such a tool is proposed and sample implementations are introduced.

Chapter 5 presents four sample networks and the simulation results thereof. To this end, the simulation tool of the previous chapter is used.

Chapter 6 recalls the results and limitations of the network model and the simulation tool used in this project. Problems are depicted and possible remedies are proposed.

Chapter 2

Theoretic Background

A sound knowledge of the wireless channel is crucial to understand wireless communications. This chapter gives a short theoretic introduction to the wireless channel. A general description including channel models is given in section 2.1. MIMO, as being important in future cellular networks, is described in section 2.2. In both sections, the channel capacity is derived. This is a good figure of merit. Even though realistic modulation and coding schemes do not achieve the capacity, they can get very close.

2.1 The Wireless Channel

Finding an accurate description of a wireless channel depends strongly on the communication system examined. An earth station satellite link experiences high delays and a predominating line-of-sight (LOS) component. On the other hand, a mobile station (MS) in a cellular network has often no line-of-sight (NLOS) to the BS and sees a multipath fading channel. The following remarks are mostly a summary of chapters 2 and 3 of [2] if not stated otherwise.

2.1.1 General Description

Let $x(t)$ be the signal sent by the transmitter and $y(t)$ the receive signal at the receiver. The transmit signal is reflected by different objects. This reflection mechanism at different objects results in various propagation paths. The ith propagation path arrives with a distinct attenuation and a distinct delay at the receiver. As a consequence, the receive signal can be written as

$$y(t) = \sum_i a_i(f,t)x(t-\tau_i(t)), \tag{2.1}$$

where $a_i(f,t)$ is the attenuation of the ith path and depends in general on the frequency f and time t. In the special case of a sufficiently narrow bandwidth, the frequency dependency can be omitted as the path is frequency flat for a transmission of sufficiently narrow bandwidth. The time dependency can be dropped if all objects in question are stationary or at least in no relative motion. The objects in question are the transmitter, receiver, reflectors, scatterers and so on. The parameter $\tau_i(t)$ describes the delay in time domain of the ith path. This delay depends commonly on the time t. The time dependency can be dropped in case of no relative motion of all objects in question.

In a multipath fading channel, different scales or types of fading can be observed. They are grouped into distinct fading characteristics depending on the movement of the receiving station with respect to the signal wavelength λ.

Pathloss: The average power attenuation due to the distance between transmitter and receiver is referred to as *pathloss*. In free space, this loss grows with the distance squared. However, an environment of absorbers, reflectors and shadowing objects can have a pathloss of higher order.

Shadowing: If a receiver moves much more than the wavelength λ of the signal, large objects, which obstruct some of the signal paths, can cause *shadowing*. This is sometimes referred to as a part of *large-scale fading*. In a shadowed region, the receive signal strength is typically very low. This phenomenon is usually not influenced by the distance between transmitter and receiver.

Small-scale fading: Lastly, if a receiver moves in the order of the carrier wavelength λ, it will experience destructive and constructive interference due to multipath fading. Commonly, such behaviour is frequency dependent.

A channel can consist of a combination of all three fading types. Figure 2.1 illustrates all three types and their relation with respect to the distance d between transmitter and receiver.

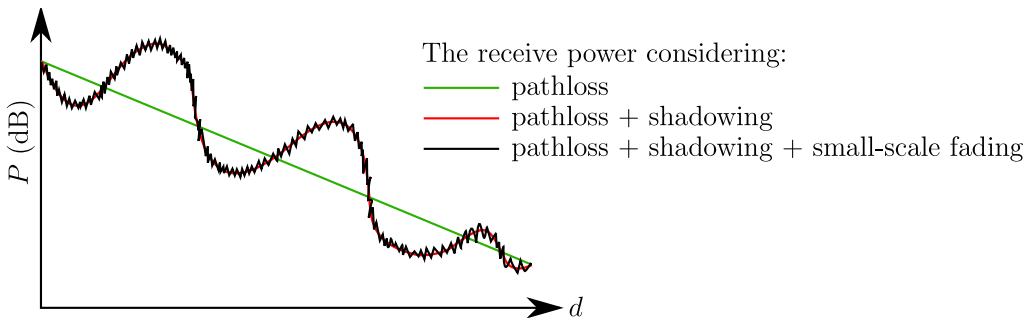

Figure 2.1: The receive power P in dB decreases linearly with the distance d. Shadowing can occur if the receiver moves multiples of the wavelength. Small-scale fading is the result of constructive and destructive interference and prevails if the receiver moves in the order of the carrier wavelength λ.

In addition, fading can be described by a few characteristic measures. Their derivation is not depicted here but can be found in [2] . These characteristic measures can be viewed as key indicators and are important in understanding the wireless channel.

Delay Spread: The time difference from the fastest (or first) to the most delayed (or last) signal path arriving at the receiver is called the *delay spread* T_d.

Coherence Bandwidth: The inverse of the *delay spread* is a measure of the frequency flatness of the channel. It is referred to as the *coherence bandwidth* W_c. It describes the amount of bandwidth over which a channel is frequency flat or, alternatively, all frequencies see the same channel.

Doppler Spread: The maximum frequency difference between different impinging waves at the receiver due to Doppler shifts is referred to as the *Doppler spread* D_s.

Coherence Time: The *coherence time* T_c is inversely proportional to the *Doppler spread*. Therefore, it is a measure of time over which the channel is time invariant or time flat.

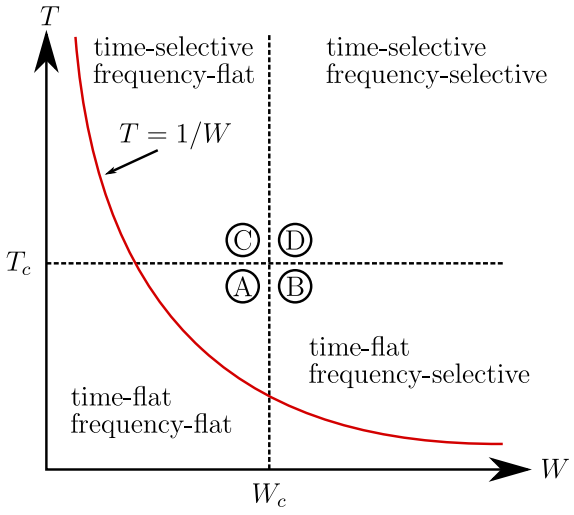

Figure 2.2: Wireless channels characterized by their fading properties.

Taking into consideration a signal of bandwidth W and burst duration T, four different channel types can be distinguished, Depending on the *coherence bandwidth* W_c and the *coherence time* T_c, see figure 2.2 [4].

Ⓐ In a system where $T \ll T_c$ and $W \ll W_c$, the channel is time-flat and frequency-flat. This is the most simple case. The channel can be represented with a constant factor h. Consequently, the input output relation is

$$y(t) = h \cdot x(t). \tag{2.2}$$

Ⓑ If $T \ll T_c$ and $W > W_c$, a time-flat and frequency-selective channel is at hand. It can be represented as a linear time-invariant (LTI) system with impulse response $h(t)$ and input output relation

$$y(t) = h(t) * x(t). \tag{2.3}$$

Ⓒ A channel is time-selective and frequency-flat if $T > T_c$ and $W \ll W_c$. It can be represented with a time varying channel gain $h(t)$ and input output relation

$$y(t) = h(t) \cdot x(t). \tag{2.4}$$

Ⓓ When $T > T_c$ and $W > W_c$, a time-selective and frequency-selective channel is at hand. This is the most general scenario.

Note that transmission below the red curve $T = 1/W$ in figure 2.2 is physically not possible. The shorter the burst duration T, the wider is the signal bandwidth W.

2.1.2 Discrete Complex Baseband Model

In wireless communications, it is often simpler to model a channel in complex baseband. Sampling the entire system at a sufficiently high rate gives a discrete complex baseband representation of the system. A rigorous derivation and discussion on this subject can be found in [1]. Consider the continuous passband representation of case Ⓒ above. Let $x[m]$ and $y[m]$ be the discrete complex baseband representations of $x(t)$ and $y(t)$, respectively, and $h_l[m]$ the channel tab at sample instant m. The input output relation can be written as

$$y[m] = \sum_l h_l[m]x[m-l]. \tag{2.5}$$

Note that $h_l[m]$ depends on m, the discrete time, and takes into account the time varying property of the channel. Furthermore, $h_l[m]$ is the lth tab of the channel. All propagation paths whose delays are close to the sampling instant contribute to the lth channel tab. Consequently, if all multiple paths are represented in one tab only, it is a frequency flat channel. Furthermore, if the channel impulse response does not depend on m either, the channel is said to be time-flat and frequency flat. This corresponds to case Ⓐ in figure 2.2.

2.1.3 Probabilistic Channel Model

In the discrete complex baseband representation of the wireless channel the unknowns of a transmitter-receiver link are the channel tab amplitude and phase and, of course, the amount of tabs needed. Assuming a fair amount of reflectors and scatterers and

path gains of random amplitudes, one can argue that the phase of each tab must follow a uniform phase distribution on the interval $[0, 2\pi)$. The amplitude of each tab is a complex circularly symmetric Gaussian random variable of zero mean. Taking this into consideration and adding a LOS component, the channel can be modeled as

$$h_l[m] = \underbrace{\sqrt{\frac{k}{k+1}}\sigma_l e^{\jmath\theta}}_{\text{LOS}} + \underbrace{\sqrt{\frac{1}{k+1}}\mathcal{CN}(0, \sigma_l^2)}_{\text{NLOS}}. \tag{2.6}$$

This channel model is referred to as a *Rician fading* channel. The factor k specifies the energy distribution between LOS path and NLOS portion of the receive signal. The special case of $k = 0$ (NLOS) is also referred to as a *Rayleigh fading* channel. The phase θ of the LOS component follows a uniform distribution on the interval $[0, 2\pi)$.

The *pathloss* in this channel model is actually the standard deviation σ_l. This value can be a function of the distance d between transmitter and receiver, the height h_t of the transmitter, the height h_r of the receiver, the center frequency f_c, and empirical constants depending on the environment. The WINNER II model as described in [8] uses different pathloss formulas, which depend on the environment. For a rural NLOS area, the pathloss PL computes as

$$\begin{aligned} PL &= 25.1\log_{10}(d) + 55.4 - 0.13\,(h_t - 25)\log_{10}\left(\frac{d}{100}\right) \\ &\quad -0.9\,(h_m - 1.5) + 21.3\log_{10}\left(\frac{f_c}{5}\right). \end{aligned} \tag{2.7}$$

Shadowing can be modeled using a log-normal distribution. Such a behaviour can be taken into account by adding a normal distributed random variable to the pathloss in dB. For example, in the WINNER II model the pathloss from equation (2.7) is modified as:

$$\sigma_l(\text{dB}) = -PL + \mathcal{N}(0, \sigma^2_{shadowing}), \tag{2.8}$$

where $\sigma^2_{shadowing}$ is an empirical value.

In addition to multiplicative disturbance (fading), additive disturbance must be accounted for, as well. Therefore, noise in the receiver structure needs to be added to the receive signal $y[m]$. White Gaussian noise $w[m] \sim \mathcal{CN}(0, N_0)$ with power spectral density (PSD) N_0 is used. Hence, the discrete complex baseband receive signal $y[m]$ takes the form

$$y[m] = \sum_l h_l[m]x[m-l] + w[m]. \tag{2.9}$$

2.1.4 Channel Capacity

Notwithstanding the discussion on how to model a channel one might be interested in the optimal performance of a communication system. In the field of information theory

the channel capacity C is a good figure of merit. Given a channel, the capacity gives a maximum data rate in terms of bits/s within a certain bandwidth for which an arbitrarily low error probability can be achieved using appropriate coding. One can still transmit above the capacity, but it will be impossible to find a coding scheme which drives the error probability to zero.

In the following, the channel capacities for three channels are represented and briefly explained. A complete derivation can be found in [2, 9].

AWGN-channel: An additive with Gaussian noise (AWGN) channel experiences no fading. The receive signal consists of the transmit signal with additive white Gaussian noise. The capacity is a function of the transmit power P and PSD N_0 of the noise, it computes as

$$C = \log\left(1 + \frac{P}{N_0}\right) \text{ bits/s/Hz.} \tag{2.10}$$

Time-flat frequency-flat fading channel: For a one tab fading channel with a fix tab, the capacity is in this case also a function of the tab gain h:

$$C = \log\left(1 + |h|^2\frac{P}{N_0}\right) \text{ bits/s/Hz.} \tag{2.11}$$

Time-selective frequency-flat fading channel: In case the channel tab h is a random variable, the capacity is limited by the smallest (worst) realization of h. Therefore, an ergodic capacity is more meaningful. It is the mean of the capacities of all realizations of h:

$$C = \mathrm{E}\left\{\log\left(1 + |h|^2\frac{P}{N_0}\right)\right\} \text{ bits/s/Hz.} \tag{2.12}$$

2.2 MIMO

The demand for higher data rates has been constantly increasing over the past few years. However, limited bandwidth and power constraints require more sophisticated communication techniques. MIMO exploits the spatial dimension of a channel. Hence, MIMO enables the use of an additional dimension besides time and frequency.

2.2.1 The MIMO Channel

Under the assumption of a frequency flat and time flat channel, as was discussed in section 2.1 about the wireless channel, the whole channel characteristics can be summed up in one discrete complex baseband channel tab h. So far, only single-input single-output

(SISO) systems with one antenna at the transmitter and one antenna at the receiver have been considered. If the receiver now uses two antennas, that are sufficiently spaced, each antenna receives a different signal due to small-scale fading processes. If one of the channels between the transmit antenna and the two receive antennas is in a deep fade, it is still possible, that the second channel is sufficiently good for reliable data transmission. This concept can be expanded to N_r receive antennas and N_t transmit antennas. Consequently the channel function h consists no longer of a single coefficient. It is a matrix $\mathbf{H} \in \mathbb{C}^{N_r \times N_t}$ of the form

$$\mathbf{H} = \begin{bmatrix} h_{11} & h_{12} & \dots & h_{1N_t} \\ h_{21} & h_{22} & \dots & h_{2N_t} \\ \vdots & \vdots & \ddots & \vdots \\ h_{N_r1} & h_{N_r2} & \dots & h_{N_rN_t} \end{bmatrix}. \tag{2.13}$$

Figure 2.3 illustrates what the individual entries h_{ij} of the channel matrix $\mathbf{H}$ represent. Basically, h_{ij} is the channel tab between transmit antenna j and receive antenna i.

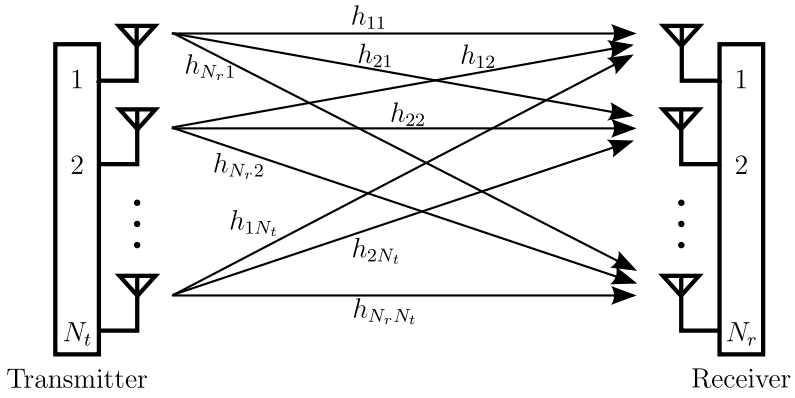

Figure 2.3: Illustration of the channels h_{ij} in a MIMO system

The input output relation of a MIMO system can be written as

$$\mathbf{y}[m] = \mathbf{H}\mathbf{x}[m] + \mathbf{w}[m], \tag{2.14}$$

with $\mathbf{x} \in \mathbb{C}^{N_t}$, $\mathbf{y} \in \mathbb{C}^{N_r}$ and $\mathbf{w} \sim \mathcal{CN}(0, N_0\mathbf{I}_{N_r})$.

2.2.2 Singular Value Decomposition

In the following discussion, $\mathbf{H}$ is assumed to be known at the transmitter as well as at the receiver. Through proper pre- and post-processing, up to n individual spatial streams can be used to transmit data, $n = \min\{N_t, N_r\}$. The channel matrix can be decomposed into three matrices, two of them rotations, the remaining a scaling. In fact, each linear transformation can be expressed as a rotation, a scaling and again a rotation. The singular value decomposition (SVD) produces exactly those three matrices.

$$\mathbf{H} = \mathbf{U}\Lambda\mathbf{V}^H \tag{2.15}$$

$\mathbf{U} \in \mathbb{C}^{N_r \times N_r}$ and $\mathbf{V} \in \mathbb{C}^{N_t \times N_t}$ are both unitary rotation matrices. If a matrix $\mathbf{A}$ is unitary, then $\mathbf{A}\mathbf{A}^H = \mathbf{A}^H\mathbf{A} = \mathbf{I}$. The matrix Λ, on the other hand, is a rectangular matrix with zeros on the off-diagonal entries. On the diagonal, the singular values of the channel matrix $\mathbf{H}$ are placed in descending order: $\lambda_{11} \geq \lambda_{22} \geq \cdots \geq \lambda_{nn}$. Note that the amount of non-zero singular values equals the rank of the channel matrix $\mathbf{H}$.

Now, if the transmitter performs the following pre-processing

$$\tilde{\mathbf{x}} = \mathbf{V}\mathbf{x}, \tag{2.16}$$

$\tilde{\mathbf{x}}$ is the new transmit signal. The receiver performs the following post-processing

$$\tilde{\mathbf{y}} = \mathbf{U}^H\mathbf{y}. \tag{2.17}$$

Furthermore, define

$$\tilde{\mathbf{w}} = \mathbf{U}^H\mathbf{w}. \tag{2.18}$$

Note that $mathbf\tilde{w}$ is still $\mathcal{CN}(0, N_0\mathbf{I}_{N_r})$ because $\mathbf{U}^H$ is unitary. The overall input output relation is

$$\begin{aligned}
\tilde{\mathbf{y}} &= \mathbf{U}^H\mathbf{y} && (2.19)\\
&= \mathbf{U}^H(\mathbf{H}\tilde{\mathbf{x}} + \mathbf{w}) && (2.20)\\
&= \mathbf{U}^H\mathbf{U}\Lambda\mathbf{V}^H\tilde{\mathbf{x}} + \tilde{\mathbf{w}} && (2.21)\\
&= \Lambda\mathbf{V}^H\mathbf{V}\mathbf{x} + \tilde{\mathbf{w}} && (2.22)\\
&= \Lambda\mathbf{x} + \tilde{\mathbf{w}}. && (2.23)
\end{aligned}$$

Equation (2.23) shows that thanks to the pre- and post-processing, n spatial data streams can be used for transmission. Note that each stream does experience a different attenuation according to its singular value. Therefore, clever power distribution over the sub-channels is necessary. Note, however, that only a full rank channel matrix can lead to n spatial data streams. This requires a rich scattering environment. Figure 2.4 gives a schematic overview of the just discussed MIMO system.

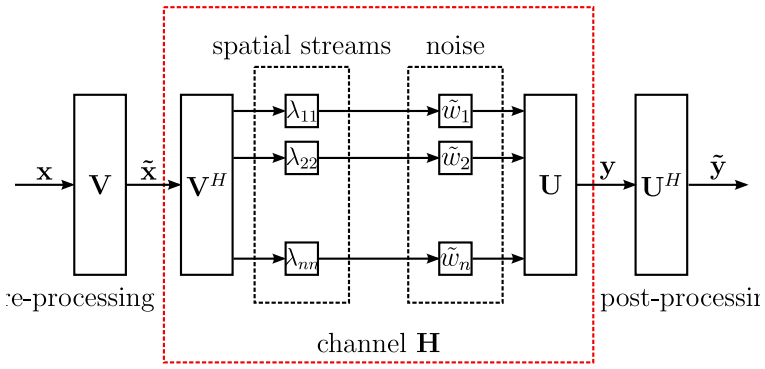

Figure 2.4: A complete MIMO system using SVD.

2.2.3 Capacity of MIMO

The SVD with proper pre- and post-processing leads to n independent parallel data streams from the transmitter to the receiver. Consequently, the capacity of such a system is the sum of the n capacities of the individual streams. The ith stream can be viewed as a SISO channel with attenuation λ_{ii}. The capacity can thus be written as

$$C = \max_{P_i} \sum_{i=1}^{n} \log \left(1 + \frac{\lambda_{ii}^2 P_i}{N_0} \right) \text{ bits/s/Hz}, \tag{2.24}$$

with P_i the transmit power allocated to the ith data stream. Note that if the channel matrix $\mathbf{H}$ has not full rank, some of the singular values λ_{ii} are zero. The power constraint $\sum_{i=1}^{n} P_i = P$ must be fulfilled. The waterfilling power allocation method fulfills this constraint and maximizes the capacity formula (2.24) above [2]. Basically, this method assigns most power to the strongest stream and less power to weaker streams.

More generally, the capacity for a MIMO channel with a fix channel matrix $\mathbf{H}$ can be computed as [3]

$$C = \sup_{\mathbf{K}_\mathrm{s}} \log_2 \det \left(\mathbf{K}_\mathrm{n} + \mathbf{K}_\mathrm{s} \right) - \log_2 \det \left(\mathbf{K}_\mathrm{n} \right). \tag{2.25}$$

$\mathbf{K}_\mathrm{n}$ is the covariance matrix of the noise $\mathbf{w}$ and $\mathbf{K}_\mathrm{s}$ is the covariance matrix of the receive signal:

$$\mathbf{K}_\mathrm{s} = \mathbf{H} \cdot \mathrm{E} \left\{ \mathbf{x} \cdot \mathbf{x}^H \right\} \cdot \mathbf{H}^H. \tag{2.26}$$

The power constraint $\mathrm{E} \left\{ \mathbf{x} \cdot \mathbf{x}^H \right\} \leq P$ must be fulfilled.

Chapter 3

Cellular Networks

A cellular network consists of fix transceiver stations called BS that communicate with mobile transceiver stations called MS. These BS provide services such as telephony or Internet connectivity to MS associated with the BS. Depending on the location of the MS, the wireless channel in cellular networks can consist of NLOS paths only. The geographic area, which is served by one BS, is a cell. There are, however, various definitions of cell size. For example, the cell size can be the geographic area in which the received power of the BS serving the cell is stronger than the receive power of other BS. The latter is also referred to as *interference*. The cell size depends strongly on interference. Of course, other aspects such as the environment, pathloss, shadowing, and so on influence the cell size as well. As many BS are placed in one geographic region, cellular networks are typically interference limited. In systems discussed in the preceding chapter, the transmitter serves one receiver only. However, in cellular networks, the BS serves various MS at the same time and appropriate multiple access methods are required.

This chapter was written to give a brief overview of a few aspects of cellular networks with emphasis on future cellular networks. Section 3.1 sets the network model and nomenclature used throughout this and subsequent chapters. Various multiple access methods can be used in cellular networks, these are depicted in section 3.2. As the capacity of a cellular network is difficult to compute, an achievable rate is discussed in the subsequent section 3.3. Furthermore, cooperative communication schemes and relaying can enhance data rate and coverage in future cellular networks as depicted in sections 3.4 and 3.5, respectively. Lastly, a motivation to simulating (future) cellular networks is presented in the last section of this chapter.

3.1 Network Model

The cellular networks in this work consist of planar areas divided into cells. Each cell is served by one BS and is sectorized into three sectors. Each sector is served by one BS part (antenna array) which is treated as an individual and fully functional BS, see figure 3.1. Additionally, relay stations (RS) can be placed in a sector. Only the downlink transmission is considered. The network consists of N_b BS and N_m MS. It is assumed that one BS serves exactly one MS ($N_b = N_m$). Each BS has an antenna array of N_t elements and each MS has N_r antennas. The transmit symbol for MS_m, $m \in \{1, 2, \ldots, N_m\}$, is denoted as $\mathbf{s}_m$ and is a random variable. It is assumed to be i.i.d. $\mathcal{CN}(0, \mathbf{I})$. The covariance matrix of $\mathbf{s}_m$ is

$$\mathrm{E}\{\mathbf{s}_m \cdot \mathbf{s}_m\} = \mathbf{I}. \tag{3.1}$$

Quasi-stationary channel matrices $\mathbf{H}_{mb}$ from BS b to MS m over the duration of one transmit symbol are assumed. They are of dimension $\mathbf{H}_{mb} \in \mathbb{C}^{N_r \times N_t}$. Each BS transmits with a maximum power of P_{BS} Watts. The transmit signal at BS_b, $b \in \{1, 2, \ldots, N_b\}$, is denoted by $\mathbf{x}_b$. It is a coded version of the transmit symbols $\mathbf{s}_m$. If serves MS_m, then

$$\mathbf{x}_b = \mathbf{G}_{mb} \cdot \mathbf{s}_m, \tag{3.2}$$

with $\mathbf{G}_{mb}$ as the pre-coding matrix at BS_b for symbol $\mathbf{s}_m$. The noise $\mathbf{n}_m$ at the MS is considered to be i.i.d. $\mathcal{CN}(0, \mathbf{I})$ with the covariance matrix $\mathbf{K}_N = P_N \cdot \mathbf{I}$, where P_N is the PSD of the noise.

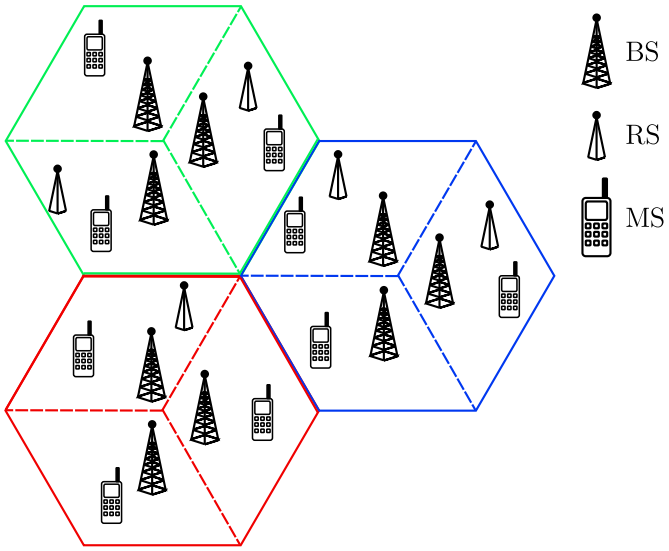

Figure 3.1: The network model: One BS serves one cell, each cell is sectorized into three sectors. The BS part in each sector is treated as an individual BS. Each BS serves exactly one MS. As an option, relays can be placed in a sector.

3.2 Multiple Access

In cellular networks, a number of multiple access methods are used. Different methods demand higher or lower complexities, respectively. But they have in common that, in the end, several MS can access one BS at the same time. They further aid to share available resources among various MS and/or BS. Multiple access can be done in time, frequency, and space:

Time: Various MS share a channel by dividing it into time slots. This can be useful in a scenario, where MS require lower data rates than the channel quality would allow. If several MS used their own frequency portions of the channel before, they now share one frequency using different time slots, other channel or frequency portions become available and more MS can be incorporated.

Frequency: If different cells use different frequency portions, they don't interfere with each other. Cells that are sufficiently distant from each other can use the same frequency portion. Such a frequency reuse approach, however, reduces the available bandwidth per cell and thus the data rate.

Space: In future cellular networks MIMO will be used. Even though this can be a rather complex technique as opposed to existing cellular networks, MIMO can boost MS data rates without using more frequencies or more time slots. In addition, multiuser-MIMO techniques are able to separate different data streams in space, so that the entire frequency or time can be used by several MS simultaneously.

3.3 Achievable Rate of a Cellular Network

In section 2.2.3 about the capacity of a single user MIMO system, the capacity formula of a MIMO communication scheme has been presented. As mentioned in the introduction to this chapter, cellular networks are to a large extent interference limited. In particular close to the cell borders, the interference of adjacent cells can be very high. There are many ways to treat the interference of other BS, one of them is to treat it as noise. As each BS serves exactly one MS, BS and corresponding MS use the same index k. Then, the rate R_k of MS k served by BS k

$$R_k = \log_2 \det \left(\mathbf{K}_\mathrm{N} + \mathbf{K}_\mathrm{I} + \mathbf{K}_\mathrm{D} \right) - \log_2 \det \left(\mathbf{K}_\mathrm{N} + \mathbf{K}_\mathrm{I} \right). \tag{3.3}$$

is achievable [2], where $\mathbf{K}_\mathrm{D}$ is the covariance matrix of the desired signal

$$\mathbf{K}_\mathrm{D} = \mathbf{H}_{kk} \cdot \mathrm{E}\left\{ \mathbf{x}_k \cdot \mathbf{x}_k^H \right\} \cdot \mathbf{H}_{kk}^H = \mathbf{H}_{kk} \cdot \mathbf{G}_{kk} \cdot \mathbf{G}_{kk}^H \cdot \mathbf{H}_{kk}^H. \tag{3.4}$$

If no pre-coding is applied, the pre-coding matrix can be reduced to the identity matrix $\mathbf{I}$ multiplied with the square root of the BS transmit power such that

$$\mathbf{K}_\mathrm{D} = \mathbf{H}_{kk} \cdot P_{BS} \cdot \mathbf{H}_{kk}^H. \tag{3.5}$$

The covariance matrix of the interfering signals $\mathbf{K}_{\mathrm{I}}$ is a summation of the single contributions of each interfering BS i. The computation is similar to the computation of the covariance matrix of the desired signal:

$$\begin{aligned}
\mathbf{K}_{\mathrm{I}} &= \mathrm{E}\left\{\left(\sum_{i\neq k}\mathbf{H}_{ik}\cdot\mathbf{x}_i\right)\cdot\left(\sum_{i\neq b}\mathbf{H}_{ik}\cdot\mathbf{x}_i\right)^H\right\} \\
&= \mathrm{E}\left\{\sum_{i\neq k}\sum_{i'\neq k}\mathbf{H}_{ik}\cdot\mathbf{x}_i\cdot\mathbf{x}_{i'}^H\cdot\mathbf{H}_{i'k}^H\right\} \\
&= \sum_{i\neq k}\sum_{i'\neq k}\mathbf{H}_{ik}\cdot\mathbf{G}_{ii}\cdot\mathrm{E}\left\{\mathbf{s}_i\cdot\mathbf{s}_{i'}\right\}\cdot\mathbf{G}_{i'i'}^H\cdot\mathbf{H}_{i'k}^H \\
&= \sum_{i\neq k}\mathbf{H}_{ik}\cdot\mathbf{G}_{ii}\cdot\mathbf{G}_{ii}^H\cdot\mathbf{H}_{ik}. \qquad (3.6)
\end{aligned}$$

The last equality holds, because $\mathrm{E}\left\{\mathbf{s}_i\cdot\mathbf{s}_{i'}\right\}=0$ for $i\neq i'$. If no pre-coding is applied, $\mathbf{K}_{\mathrm{I}}$ reduces to

$$\mathbf{K}_{\mathrm{I}}=\sum_{i\neq k}\mathbf{H}_{ik}\cdot P_{BS}\cdot\mathbf{H}_{ik}. \qquad (3.7)$$

3.4 Cooperative Communication

As mentioned in the introduction to this chapter, communication in cellular networks can be strongly interference limited and resources such as frequency are shared among MS and/or BS. Figure 3.2 (a) shows a simple example setup with two MS and two BS. MS_1 is connected with BS_1 and MS_2 is connected with BS_2. MS_1 and MS_2 receive with the rates R_1 and R_2, respectively. Both BS use the same frequency. If BS_1 transmits and BS_2 is silent, MS_1 has rate $R_{1,max}$. On the other hand, if BS_2 transmits and BS_1 is inert, MS_2 receives with rate $R_{2,max}$. When both BS are transmitting alternately using time slots, then none of the MS will achieve the maximum possible rate as if only one BS where transmitting. But every point on the line in figure 3.2 (b) can be achieved. A fair point of operation is achieved when $R_1=R_2$ as indicated in the same figure.

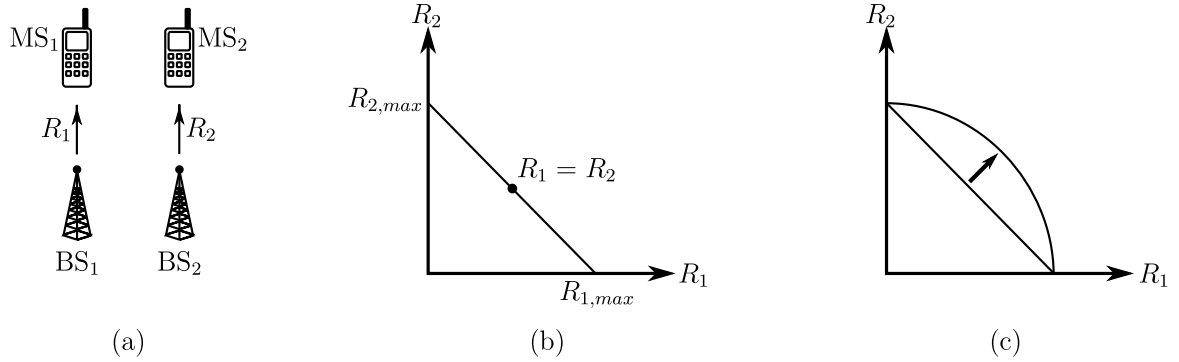

Figure 3.2: (a) Two BS two MS setup. (b) Two BS two MS system without cooperation using time slots. (c) Two BS two MS system with cooperation.

Now, cooperative communication takes advantage of the fact that both MS receive the signal from both BS. If both BS know the channels from each BS to each MS and also the intended signals for the two MS, then the rate curve in figure 3.2 (b) can be stretched outwards as in figure 3.2 (c).

There exists a vast amount of algorithms and methods which implement cooperation in a cellular network. This is also subject to current research. Some cooperation algorithms portion equal rates to all MS in the cooperation area. As an example, a method achieving the same rate for all MS in a corporation area is presented. It incorporates *block diagonalization*, which eliminates interference from cooperating BS. This is only optimal in the high SNR regime (SNR $\rightarrow \infty$).

In a network where all BS cooperate, the transmit signal $\mathbf{x}_b$ at BS b is now a summation of all pre-coded transmit symbols $\mathbf{s}_m$:

$$\mathbf{x}_b = \sum_{m=1}^{N_m} \mathbf{G}_{mb} \cdot \mathbf{s}_m. \tag{3.8}$$

The receive signal $\mathbf{y}_m$ at MS m is then:

$$\mathbf{y}_m = \underbrace{\sum_{b=1}^{N_b} \mathbf{H}_{mb} \cdot \mathbf{G}_{mb} \cdot \mathbf{s}_m}_{\text{desired signal}} + \underbrace{\sum_{b=1}^{N_b} \sum_{j \neq k} \mathbf{H}_{mb} \cdot \mathbf{G}_{jb} \cdot \mathbf{s}_j}_{\text{intra-cooperation interference (ICI)}} + \mathbf{n}_m. \tag{3.9}$$

The pre-coding matrices $\mathbf{G}_{mb}$ must be chosen such that the desired signal in equation (3.9) is not zero but that the ICI is zero. In detail, this means that:

$$\mathbf{H}_{mb} \cdot \mathbf{G}_{mb} \neq 0 \quad , b \in \{1, 2, \ldots, N_b\} \tag{3.10}$$

$$\mathbf{H}_{mb} \cdot \mathbf{G}_{jb} = 0 \quad , \forall \quad j \neq m, b \in \{1, 2, \ldots, N_b\}. \tag{3.11}$$

Equation (3.10) holds if the channel matrices are drawn according to a non-degenerate continuous distribution. Equation (3.11) requires the pre-coding matrices $\mathbf{G}_{mb}$ to be computed as:

$$\mathbf{G}_{mb} = \text{null} \left\{ \begin{bmatrix} \mathbf{H}_{1b} \\ \mathbf{H}_{2b} \\ \vdots \\ \mathbf{H}_{(m-1)b} \\ \mathbf{H}_{(m+1)b} \\ \vdots \\ \mathbf{H}_{N_m b} \end{bmatrix} \right\}. \tag{3.12}$$

Where $\mathbf{B} = \text{null}\{\mathbf{A}\}$ returns a basis $\mathbf{B}$ of the null space of $\mathbf{A}$ such that $\mathbf{B} \cdot \mathbf{A} = \mathbf{0}$. Thus, equation (3.11) is fulfilled. This eliminates ICI and the MS_m only receives the desired signal $\mathbf{s}_m$ from all cooperating BS.

In addition, the matrices $\mathbf{G}_{mb}$ need to be scaled for two reasons:

1. The maximum power P_{BS} per BS must not be exceeded.

2. The power over the pre-coding matrices should be distributed such that each MS in the cooperation area receives a certain amount of power. This is necessary due to some MS having bad channels and other MS having good channels. In this example, each MS is supposed to have the same rate at the end.

By dividing the pre-coding matrices into a normalized matrix $\tilde{\mathbf{G}}_{mb}$ and a scaling matrix $\mathbf{Q}_m$ as

$$\mathbf{G}_{mb} = \tilde{\mathbf{G}}_{mb} \cdot \mathbf{Q}_m, \tag{3.13}$$

the following optimization problem can be defined:

$$\max_{\mathbf{Q}_m} \min\{R_1, R_2, \ldots, R_{N_m}\}, \tag{3.14}$$

$$\text{such that} \qquad \mathrm{Tr}\left\{\sum_{m=1}^{N_m} \mathbf{G}_{mb} \cdot \mathbf{G}_{mb}^H\right\} \leq P_{BS} \qquad \forall \quad b \in \{1, 2, \ldots, N_b\} \tag{3.15}$$

If the optimization does not reach a specified target rate, one or more MS can be omitted. The max min optimization achieves the same rate for all MS in the cooperation area. There are other approaches, i.e. the maximization of the sum rate and so on.

3.5 Relay Stations

One feature to future cellular networks is the deployment of RS beyond simple repeaters. There are numerous implementation forms of RS. They are supposed to be less complex than a BS, otherwise it would be more convenient to deploy more BS in a network than adding RS. Advantageously, RS are geographically placed such that they have a good connection to a BS, for example a LOS path. RS can be deployed to extend cell sizes or to cover regions in a network, where coverage is constantly shadowed or poor.

As an example, a simple *decode and forward* technique is explained here. The basic setup is depicted in figure 3.3. The BS has a direct link to the MS with link rate R_d if the RS is silent. A second link from BS to MS via RS with link rates R_1 between BS and RS and R_2 between RS and MS gives an alternative connection. The transmission over the two links (BS-RS and RS-MS) via RS does not happen simultaneously. In a first step, the BS transmits to the RS while the RS transmission is inert. In a subsequent step, the BS is silent and the RS transmits the just received data to the MS. Allowing both transmissions to take equally long, the total achievable rate R_{RS} on this alternate link is then

$$R_{RS} = \frac{1}{2} \min\{R_1, R_2\}. \tag{3.16}$$

However, this equal time allocation is not optimal. A better time allocation t_1 for R_1 and t_2 for R_2 can be found solving the optimization problem

$$R_{RS} = \max_{t_1,t_2} \min \{t_1 R_1, t_2 R_2\} . \tag{3.17}$$

Equation (3.17) must comply with the constraint $t_1 + t_2 = 1$. After the optimization, the MS decided the following way:

$$\text{MS chooses} \begin{cases} \text{direct link} & \text{if } R_d \geq R_{RS}, \\ \text{link via RS} & \text{if } R_d < R_{RS}. \end{cases}$$

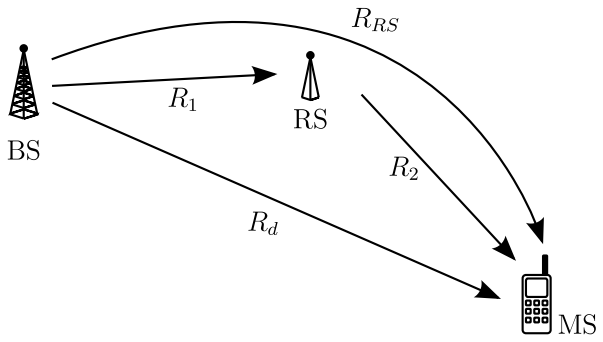

Figure 3.3: Sample topology with BS, RS and MS.

3.6 Simulating Cellular Networks

Having gone through all the mathematical formulae in the past sections and chapters, the need for simulating cellular networks might not be so inherent. There are, however, several reasons why simulations are indispensable.

- In an arbitrary cellular network setup, capacity computations are very difficult. Using the achievable rate instead simplifies the matter to some extent. However, channel matrices from all BS to all MS need to be computed. In addition, RS and cooperation need to be considered as well. And what's more, different cooperation schemes and RS techniques need to be computed separately for performance analysis and comparison of different schemes.

- As the channel matrices are usually modeled as random variables as described in section 2.1.3, meaningful results such as achievable rates can only be computed by repeating a simulation numerous times and then averaging the results. The frequent repetitions have also the effect that aspects such as a time-selective channel can be simulated using a time-flat channel only.

- A generic modularly built simulation environment, which allows for arbitrary setups, is needed. Using different RS techniques, different cooperation schemes, and so on, as building modules of a tool, allow to simulate arbitrary combinations of several methods. This is important for a good evaluation of different techniques.

For the above mentioned reasons, a generic simulation environment is necessary. As it is arduous work to program a simulation framework for each network individually, it should be as generic as possible. This means that it should be able to process and simulate any arbitrary cellular network. Furthermore, a intuitive preparation unit and an extensive analysis unit accompanying the actual simulation can improve the usability tremendously and reduce programing time to a large extent.

Chapter 4

Simulation Tool

The simulation tool developed in this project will be presented in this chapter. As mentioned in section 3.6 of the previous chapter, a generic simulation tool is necessary to understand and analyze (future) cellular networks. Section 4.1 of this chapter gives a logical overview of a simulation tool and its features. It is depicted how a simulation environment can be split into logical building blocks, each having distinct functions and meeting different requirements.The subsequent sections 4.2, 4.3, and 4.4 provide sample implementations of these building blocks. Lastly, section 4.5 illustrates limitations of this simulation tool. Even though the entire tool was programmed in Matlab, no code shall be presented in this report.

4.1 Conceptual Layout

A generic simulation tool is most useful, if it is built in a modular fashion. This inherently means that the tool is structured into replaceable blocks. This allows the user to substitute individual blocks and, what's more, to add blocks and thus enhancing the functionality of the tool. Such a conceptual and modular layout is depicted in figure 4.1. The three basic building blocks are:

- The *Preparation* block is required to allow the user to setup an arbitrary network layout and should provide a simple user interface. A sample *Preparation* block is depicted in section 4.3 of this chapter.
- The *Simulation* box is the heart of the simulation tool. It performs the actual simulation according to the parameters it receives from the *preparation* block and hands the results down to the *Analysis* block. The *Simulation* box is subdivided into three individual modular parts:
  - The *Simulation Engine* takes the values from the *Preparation* block. It is

required to manage the entire simulation procedure and call upon other blocks if necessary. The results are handed down to the *Analysis* block.

- The *Channel* block receives parameters from the *Simulation Engine* and returns channel matrices.
- The *Rate* block receives parameters such as channel matrices from the *Simulation Engine* and computes the data rate according to the scheme in use and returns the result.

A sample implementation of these three blocks is depicted in section 4.2.

- As a final block, an *Analysis* tool is necessary to facilitate interpretation of the simulation results. Each sub-block provides a certain means of analysis. A sample *Analysis* block is described in section 4.4 of this chapter.

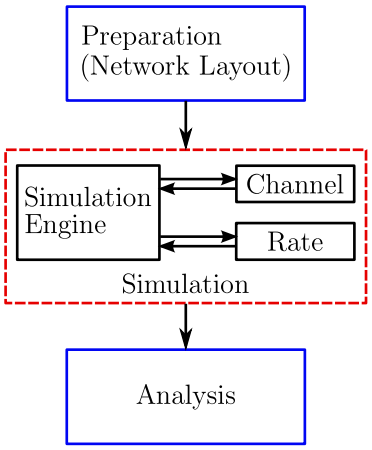

Figure 4.1: Conceptual layout of the simulation tool for cellular networks. The simulation tool is divided into *Preparation*, *Simulation*, and *Analysis*.

4.2 Simulation Block

As briefly explained in the preceding section, the simulation block can be spit up into three blocks, the *simulation engine*, the *channel*, and the *rate* block.

4.2.1 Simulation Engine

The simulation engine is the heart of the simulation block. Apart from controlling the other two blocks within the simulation block, it performs the following tasks: It places MS in the simulation area and then calls the channel block to produce the corresponding channel matrices and subsequently calls the rate block. As mentioned in previous chapters, in this project each BS serves exactly one MS. Therefore, only one test MS is placed and

all BS are assumed to be transmitting at full power. Conversely, if RS are involved, some of the RS are turned off with a certain probability (see section 4.3 for more details).

On the other hand, If there are cooperating sectors in a topology, in a first step, geographical borders are computed for each cooperating sector according to figure 4.2. This corresponds to the area where a MS is forced to connect with the area's corresponding BS. This is necessary for the following reason. In a topology without cooperation, each BS is assumed to serve exactly one MS and to be transmitting at full power. As a consequence, there are as many MS in the cooperation area including the test MS as there are cooperating BS, each pertaining to one sector's area. As all channel matrices from each cooperating BS to each MS must be known, the geographic location of each MS needs to be known. This is necessary, as the channel matrices depend on the distance and angle between BS and MS. Therefore, if the test MS enters the area of a cooperating sector, other MS are chosen randomly in the other cooperating sector areas so that each cooperating sector has one MS in its area. With the additional information of MS position, the channel block is called in order to produce the desired channel matrices. As a next step the rate block is called to compute the achievable rate using the channel matrices from the previous step.This entire process is repeated until a repetition parameter given by the preparation block is reached and the results are handed down to the analysis block. In this project, the results are not handed directly to the analysis tool, an intermediate step of saving the results to files is used.

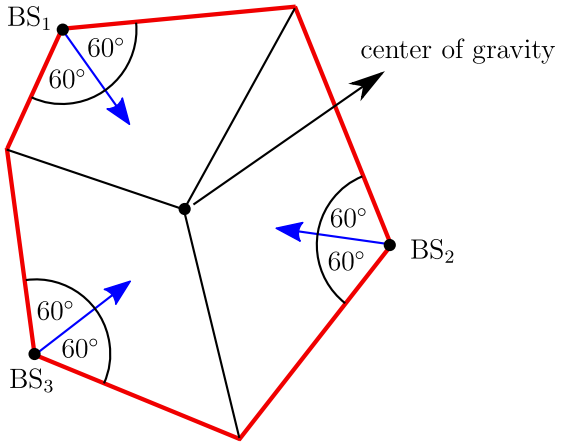

Figure 4.2: Computation of the sector borders. The blue arrows indicate the main beam direction of each BS. The center point is the center of gravity of the red revolved area.

4.2.2 Channel

The development of the channel model was not part of this project. Nevertheless, for the sake of completeness it is discussed here briefly. The implementation is based on the WINNER II channel model citewinner. A one tab time-invariant channel model was used with the properties as mentioned as an example in section 2.1.3 about probabilistic channel models. The channel depends on:

- distance d between BS and MS,
- BS height h_b,
- environment,
- propagation condition,
- radiation pattern,
- antenna correlation, and
- the center frequency f_c in GHz.

As a first step, the pathloss $Pl_{environment}$ is computed. Under a NLOS propagation condition, this is

$$\begin{aligned} PL_{urban} &= (44.9 - 6.55\log_{10}(h_b))\log_{10}(d) + 34.46 + 5.83\log_{10}(h_b) + 23\log_{10}\left(\frac{f_c}{5}\right) \\ PL_{residential} &= (44.9 - 6.55\log_{10}(h_b))\log_{10}(d) + 31.46 + 5.83\log_{10}(h_b) + 23\log_{10}\left(\frac{f_c}{5}\right) \\ PL_{rural} &= 25.1\log_{10}(d) + 55.4 - 0.13(h_b - 25)\log_{10}\left(\frac{d}{100}\right) \\ &\quad -0.9(h_m - 1.5) + 21.3\log_{10}\left(\frac{f_c}{5}\right) \end{aligned}$$

Secondly, shadowing is taken into account as described in section 2.1.3. With this information, a channel matrix $\tilde{\mathbf{H}}$ is chosen randomly using a circular Gaussian distribution with standard deviation $\sqrt{PL_{environment}}$. Subsequently the antenna correlation is taken into account by multiplying $\tilde{\mathbf{H}}$ with correlation matrices $\mathbf{Q}_t$ and $\mathbf{Q}_r$ at the transmitter and receiver, respectively. Lastly, the transmit and receive radiation pattern is included by again multiplying the channel with the patterns Pat_t and Pat_r for receiver and transmitter, respectively. The channel matrix $\mathbf{H}$ is then

$$\mathbf{H} = \mathrm{Pat}_t \cdot \mathbf{Q_t} \cdot \tilde{\mathbf{H}} \cdot \mathbf{Q_r} \cdot \mathrm{Pat}_r \tag{4.1}$$

The same channel model is used to generate all required channel matrices. This includes links from BS to MS, from BS to RS, from RS to MS and from RS and RS. RS use the same antenna radiation pattern as BS. MS are assumed to use omni-directional antennas.

4.2.3 Rate

Depending on the network topology, the rate block performs different types of rate calculations. The three types implemented in this project are explained in the following paragraphs.

No Cooperation, No Relaying

The computation of the achievable rate R_k uses formula (3.3), it is repeated here as

$$R_k = \log_2 \det \left(\mathbf{K}_\mathrm{N} + \mathbf{K}_\mathrm{I} + \mathbf{K}_\mathrm{D} \right) - \log_2 \det \left(\mathbf{K}_\mathrm{N} + \mathbf{K}_\mathrm{I} \right). \tag{4.2}$$

In case of a frequency reuse scheme with more than just one frequency, only BS using the same frequency portion are considered as interference, whereas other BS are ignored. The rate is computed over all BS and then its maximum is chosen as the achievable rate. In addition, the sector responsible for this maximum is returned to the simulation engine together with the rate. However, this procedure is very optimistic. It shows the potential of macro diversity without cooperation.

In case of a frequency reuse scheme with more than one frequency portion, the achievable rate is subsequently divided by the amount of different frequency parts. This is necessary for a quantitative comparison of different frequency reuse schemes.

Cooperation, No Relaying

The *yalmip* [5] optimization framework is used together with the SDPT3 [6] (second order cone and semi-definite programming solver) to do the optimization described in section 3.4. The rate per MS m in the cooperation area neglecting interference from non-cooperating sectors computes as

$$R_m = \log_2 \det \left(\mathbf{K}_\mathrm{N} + \mathbf{K}_D^{(m)} \right) - \log_2 \det \left(\mathbf{K}_\mathrm{N} \right). \tag{4.3}$$

However, *yalmip* is not able to optimize with the expression in equation 4.3 Therefore, a modified rate $\tilde{R}_m$

$$\tilde{R}_m = \mathrm{geomean} \left(\mathbf{I} + 1/P_n \mathbf{K}_D^{(m)} \right) \tag{4.4}$$

is used instead. Optimizing using $\tilde{R}_m$ instead of R_m gives the same $\mathbf{Q}_m$ [10]. Furthermore, looking at the desired signal covariance matrix $\mathbf{K}_D^{(m)}$ of MS_m

$$\mathbf{K}_D^{(m)} = \sum_{b=1}^{N_{B,cooperating}} \mathbf{H}_{mb} \cdot \tilde{\mathbf{G}}_{mb} \cdot \underbrace{\mathbf{Q}_m \cdot \mathbf{Q}_m^H}_{\tilde{\mathbf{Q}}_m} \cdot \tilde{\mathbf{G}}_{mb}^H \cdot \mathbf{H}_{mb} \tag{4.5}$$

and using $\tilde{\mathbf{Q}}_m$ instead of $\mathbf{Q}_m$, the optimization process is accelerated and looks now like this:

$$\max_{\tilde{\mathbf{Q}}_m} \min\{\tilde{R}_1, \tilde{R}_2, \ldots, \tilde{R}_{N_m}\} \tag{4.6}$$

This optimization problem can be solved faster because $\tilde{\mathbf{Q}}_m$ is hermitian and therefore conjugate complex symmetric with real values on the diagonal, which implies less optimization variables.

No Cooperation, Relaying

A *decode and forward* technique is used for RS. The use of RS requires a slightly different approach in order to compute the achievable rate as opposed to a topology without RS. In a first step, RS are turned off according to the state probability of RS set in the preparation tool (see section 4.3 for more details). In a subsequent step, the rate R_{BS} between BS and MS is computed. All RS, except the one associated with the BS in question, are taken into account for as interference. Therefore, the interference covariance matrix is

$$\mathbf{K}_{\mathrm{I}}^{(m)} = \sum_{b=1}^{N_{b,interfering}} \mathbf{H}_{bm}^{(\mathrm{BS})} \cdot P_{BS} \cdot \mathbf{H}_{bm}^{(\mathrm{BS})H} + \sum_{r}^{N_{r}s,interfering} \mathbf{H}_{rm}^{(\mathrm{RS})} \cdot P_{RS} \cdot \mathbf{H}_{rm}^{(\mathrm{RS})H}. \tag{4.7}$$

As a next step, the rates R_1 between each RS and its associated BS is computed using the exact same approach, just adjusting the BS and RS interference accordingly. And, as a last step regarding rate computation, the rates R_2 between each RS and the MS is computed. During this step the BS associated with the RS in question is turned off.

After having computed all the rates, an optimization problem as described in section 3.5 needs to be solved. The mentioned optimization results in a simple system of linear equations:

$$t_1 R_1 = t_2 R_2 \tag{4.8}$$
$$t_1 + t_2 = 1. \tag{4.9}$$

This optimization is computed for each BS-RS-MS link. As a final step, the maximum is taken over all rates between BS and MS directly and BS-MS-RL links. The sector responsible for this maximum rate and (if applicable) the RS responsible are returned to the simulation engine.

4.3 Preparation Block

The preparation block was implemented as a graphical user interface (GUI) and is arranged into three sections, see figure 4.3 for an example. The top part allows the user to select five distinct preferences groups organized as tabs. These are *Channel*, *Area*, *BS*, *RS*, and *MS*. The middle section displays the actual selection according to the tab. The bottom section provides a few general interfaces. These are

Simulation Name: The simulation can be assigned a name in this field.

Topology Map: A plot of the current network topology is displayed, see section 4.4 for more details. This also saves the current preferences using the name in the *Simulation Name* field.

Start Simulation: The simulation will be performed immediately. The name in the *Simulation Name* field is used to store the settings and serves a a prefix for result files.

Save Settings: The current settings are saved using the name in the *Simulation Name* field. This is helpful in case a batch job simulation cluster is used or when settings need to be modified at a later time.

Load Settings: The settings saved with the name in the *Simulation Name* field are loaded.

Reset All: This equals restarting the program.

Exit: Exits the program, data is not saved.

In the following, the five different preference tabs are explained.

Channel Tab

The first tab allows the user to set channel parameters, see figure 4.3, and consists of two boxes:

General Settings: In the top level box, the following can be set:

Environment: The environment, which the channel should model, can be specified here. Possible options are *Urban*, *Rural* and *Residential*.

Channel Model: The channel model can be selected in this pop-up menu. Possible selections are *Flat* or *Frequency Selective*. Note that the latter has not been implemented in the simulation code.

Antenna Correlation: The antenna correlation flag can be set here. Naturally, this is only significant if more than one antenna are placed in an array. The number of antennas are set in the *BS*, *RS* and *MS* tabs, respectively.

Propagation Condition: In the lower box, the conditions *LOS*, *NLOS*, and *LOSProb* can be set for individual links. These are BS-ML, BS-RL, RL-MS and RL-RL. The reason why only links with MS or RS as receiver are considered, lies in the fact that only downlink simulations are performed by the simulation block.

Area Tab

This tab consists of one box only, see figure 4.4:

General Settings: The area size can be set here, all values are in meters.

BS Tab

As a next step, all preferences regarding BS are made. This tab is structured using three boxes. Note that sectorization is used. This means that each BS is split into three sectors. In the simulation, each sector is then treated as an individual BS.

General Settings: In the top level box, settings regarding all BS can be set:

Transmit Power: The transmit power in Watts per sector can be set here.

Transmit Antennas: Each sector uses the here specified number of transmit antennas.

Center Frequency: The center frequency in GHz of the cellular network is needed. This information is necessary as the channel model depends on the center frequency.

Frequency Reuse Scheme: Either *Reuse 1* or *Reuse X* can be chosen in this pop-up menu. *Reuse 1* assigns the same frequency portion to all BS. *Reuse X* on the other hand allows the user to assign manually a desired frequency portion to each BS.

Cooperative Communication: Three options are available: *None*, *MaxTOTRate* and *MaxMinRate*. Naturally, the option *None* means no cooperation. *MaxTOTRate* uses a method, which maximizes the sum of all rates of the MS in the cooperation area. This method has not been implemented further in this project. Lastly, *MaxMinRate* uses an approach as described in section 3.4 and again in section 4.2.3. It allows to set a threshold value in the *Threshold* field. In case one of the rates after the optimization (considering all interference) lies below this thresholds, the MS with the lowest rate is omitted and the optimization is repeated. This process is iterated until all rates are above the threshold or only one MS is left.

BS Layout: Here, the geographical positions can be declared. The pop-up menu on the left allows for a set of automated setups. Note that each BS added consists of three sectors or BS with an angular spacing of 120 degrees between them. The predefined setups from the pop-up menu require a value from the *Spacing* field with the exception of the *Manual* selection. The different setups operate as follows.

3 BS pseudo-symmetric: This setup sets three BS in a pseudo-symmetric manner according to the distance d specified in the *Spacing* field on the right. The name pseudo-symmetric is due to the geographical distribution as can be seen in figure 4.5 (a). All three BS have equal rotation and height according to the *Rotation* and the *Height* field on the right. The area size as set in the *Area* tab is automatically enlarged if necessary. This setup is interesting, because it is a small symmetric scenario where cooperation of three BS pointing at each other is possible.

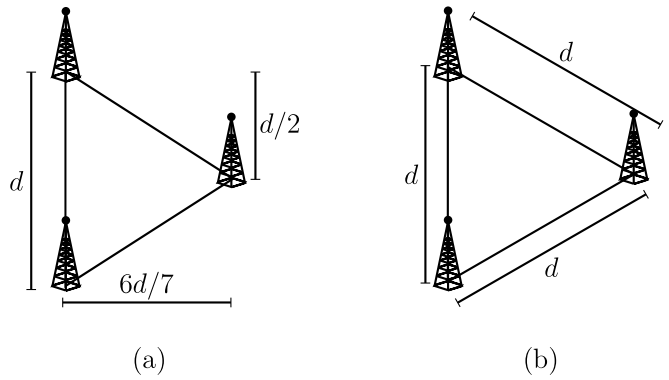

Figure 4.5: (a): The *3 BS pseudo-symmetric* setup using spacing d. The distance $6d/7$ is a consequence of a rounding procedure. (b): The *Symmetric* setup using the same spacing d.

7 BS pseudo-symmetric: This option is an expansion of the *3 BS pseudo-symmetric* to seven BS. This setup allows for a center BS being encircled by BS without a gap.

12 BS pseudo-symmetric: As above, this option is an expansion of the *3 BS pseudo-symmetric* setup to twelve BS. This setup allows three cooperating BS in the center. The cooperation area is exposed to full interference all around.

Symmetric: Conversely to the previous pseudo-symmetric setups, this option fits as many BS into the simulation area as possible using the *Spacing* field. The distances d between BS are different as opposed to the pseudo-symmetric arrangements, see figure 4.5 for more details.

Manual: This is the most flexible option. The user is able to freely place BS by setting the y and x coordinates for each BS individually. Furthermore, rotation and height can be set for each BS independently.

Note that different options can be combined, i.e. it is possible to add three BS using the *3 BS pseudo-symmetric* option and afterwards switch to *Manual* mode and add more BS. It is important to note that the *Rotation* field measures the angle clockwise off the y-axis.

BS List: Finally, after placing a BS, it will appear in the list box named *BS* together with its sectors in the *Sector* list box. The *Remove BS* and *Remove All* buttons can be used to make further corrections. In case *Reuse X* was selected in the *General Settings* box, frequencies can be assigned to each sector in the *Additional Settings* area. Similarly, in case cooperation has been selected, sectors can be added or removed to the cooperation group. Note that only one cooperation group is possible per simulation.

RS Tab

The *RS* tab as depicted in figure 4.7 is structured in a similar way as the *BS* tab. One notable difference is that a RS can have one, two, or three sectors and the rotation angle

can be set individually for each sector.

General Settings: These settings apply to all RS.

Transmit Power: The maximum transmit power in Watts per sector per RS can be set here.

Antennas per Sector: The amount of antennas per array in a sector can be modified here.

State of Relays: This option allows the user to define whether all RS should be transmitting continuously or only with probability p. It is self-evident that using the pop-up menu option *All On* equals *On With Probability* p if $p = 1$.

RS Layout: As opposed to the *BS* tab, no automated placing procedure is available for RS. This allows the user to position all RS individually and manually. As mentioned above, the number of sectors can be selected manually and the rotation angle of each sector can be selected arbitrarily. The angle is measured clockwise off the y axis.

RS List: As soon as a RS is added it appears in the RS list with its sectors. Apart from removing RS with the *Delete RS* or *Delete All RS*, their association with a BS sector can be set. This association procedure connects a RS with a BS sector. If a RS has more than one sector, each one of them is associated with the same BS sector. If this is not desired, several individual RS need to be placed at the same geographic location and associated with different BS sectors. Note that it is not possible or necessary to assign a frequency to each RS, as it automatically inherits the frequency settings from its associated BS sector.

MS Tab

The last tab (figure 4.8) is an interface for the MS settings and consists of two boxes.

General Settings:

Receive Antennas: The amount of receive antennas can be specified here.

Noise Variance: The noise variance in Watts for the additive white Gaussian noise can be set.

Repetitions for Averaging: This value gives the number of repetitions that should be simulated on each point on the grid.

Simulation Grid:

Step Size: The step size of the test MS.

Simulation Area: The test MS can be placed either in the *Whole Area* or just inside a *Polygon*. The latter can consist of up to eight vertices which can be specified individually.

4.4 Analysis Block

The analysis of simulation results is a subsequent step to simulation. To this end, a GUI analysis tool has been developed in order to simplify this endeavour, see figure 4.9. In the top field, the simulation name can be specified. The other boxes are explained in the following paragraphs.

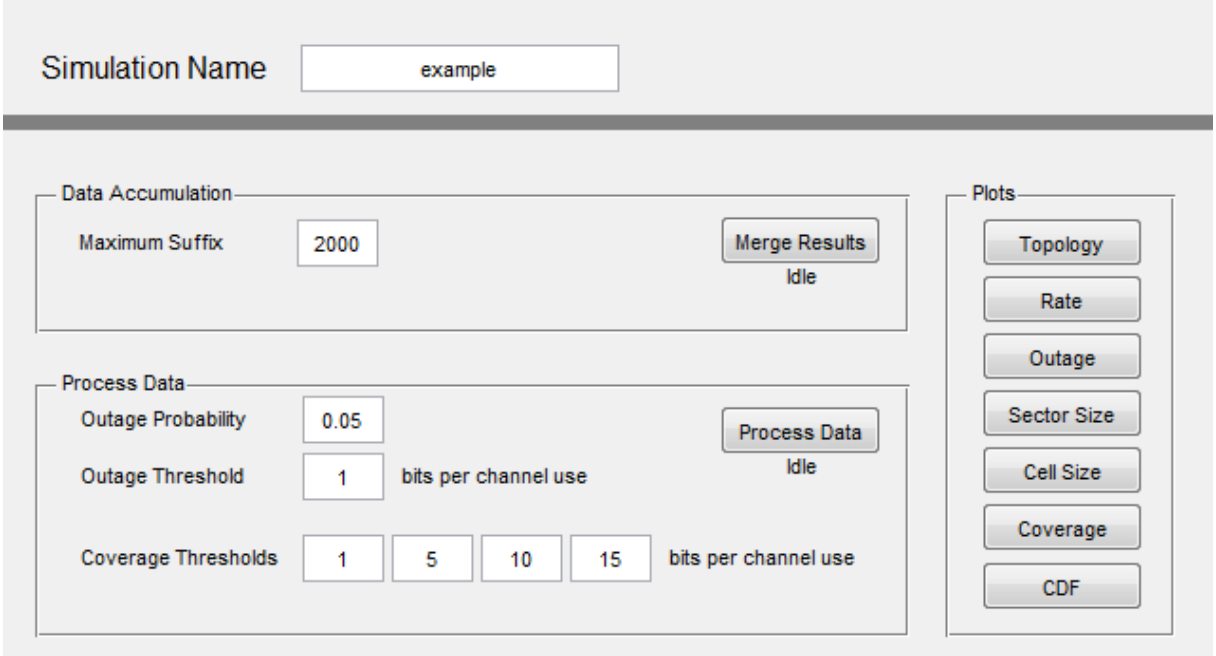

Figure 4.9: Screenshot of the analysis tool.

Data Accumulation: Often, the same simulation is run in parallel and the results need to be accumulated or merged. A maximum file name suffix number can be specified. Depending on the amount of parallel simulations, the accumulation process might take a long time. Therefore, the user is notified by a text string below the *Merge Results* button about the status of the merging procedure.

Process Data: The simulation results need to be processed before any plots can be generated. A few options are available. The outage probability needs a probability and a threshold in order to be computed correctly. Furthermore, four different coverage thresholds can be defined, in order to compute coverage areas of different data rates. Note that negative threshold values are neglected.

Plots: The now processed data can be plotted. The following plots are available: *Topology*, *Rate*, *Outage*, *Sector Size*, *Cell Size*, *Coverage*, and *CDF*. Sample plots with a brief explanation are given below:

Topology: The Topology plot is self-explanatory. BS are represented with black circles and RS with black triangles. Sectors are indicated with the radiation

pattern. Sectors using the same frequency are plotted using the same color, see figure 4.10.

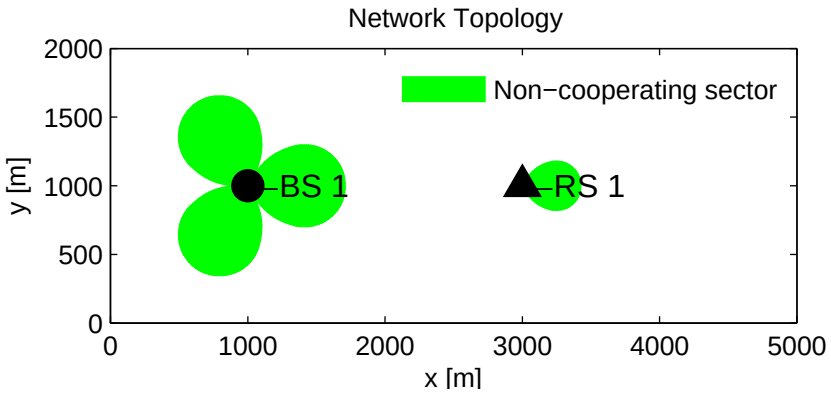

Figure 4.10: Network topology of a simple setup with one BS and one RS

Rate: The rate plot illustrates the mean rate, which is achievable, in bits per channel use. Aspects, such as the radiation pattern can be spotted, see figure 4.11. This is the achievable rate of the topology in figure 4.10 with 2000 repetitions per simulation point.

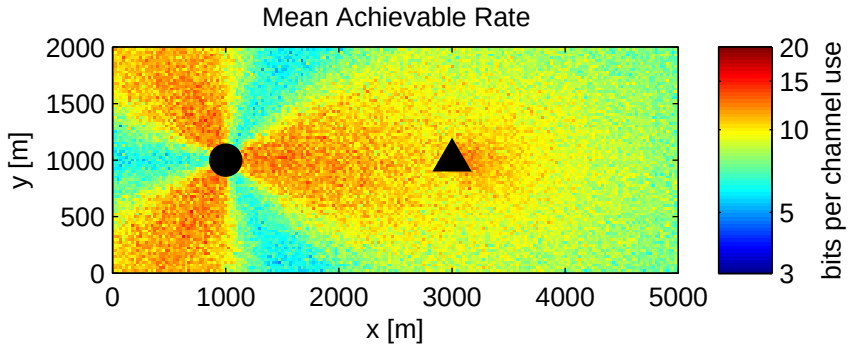

Figure 4.11: Achievable rate of the topology in figure 4.10 with 2000 repetitions per simulation point.

Outage: The outage displays the pth percentile for each simulation point. This means that $p\%$ of all achievable rate values lie below the displayed rate. In addition, a minimum threshold can be set. See figure 4.12 for an example using the topology in figure 4.10.

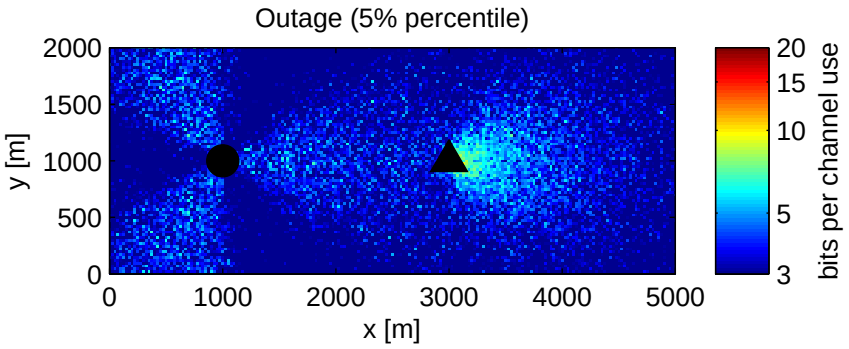

Figure 4.12: Outage with a minimum threshold of 0 bits per channel use and 5% percentile.

Sector Size: The sector, to which the test MS connected most during the simulation, is displayed using this plot.

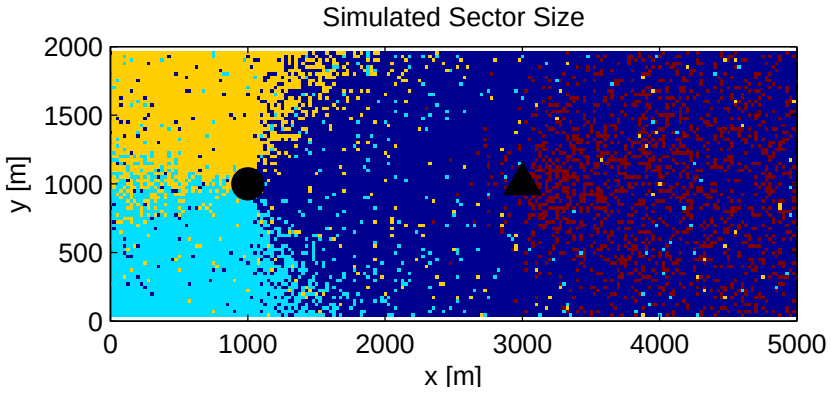

Figure 4.13: Simulated sector size of the topology in figure 4.10. BS as well as RS sectors are displayed.

Cell Size: The cell size plot is an extension of the sector size plot. All three BS sectors belonging to the same BS are displayed as one cell. Similarly, all sectors belonging to the same RS are displayed as one RS cell.

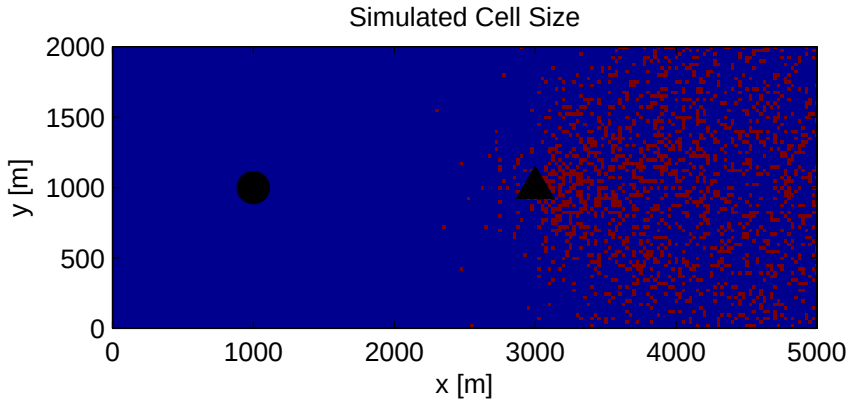

Figure 4.14: Simulated cell size of the topology in figure 4.10. BS as well as RS sectors are displayed.

Coverage: The coverage plot displays areas of the same minimum mean rate, see figure 4.12 for the coverage of the network topology in figure 4.10

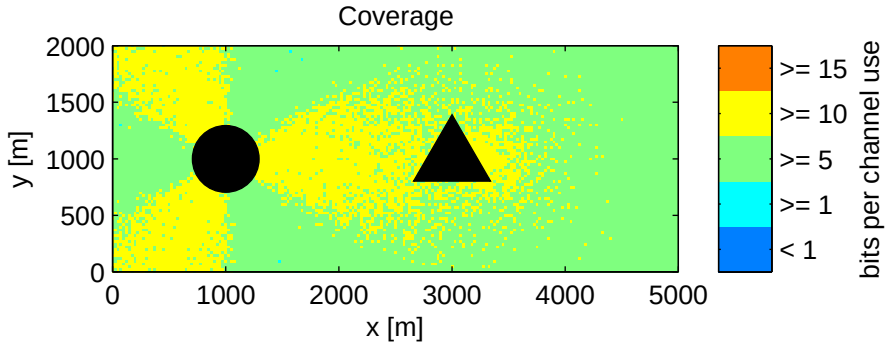

Figure 4.15: Coverage with four thresholds at one, five, ten, and 15 bits per channel use.

CDF: The cumulative distribution function (CDF) displays the cumulative probability p that all achievable rate values R lie below a certain value r:

$$CDF(r) = \mathrm{P}[R \leq r]$$

A CDF of the topology in figure 4.10 is illustrated in figure 4.16.

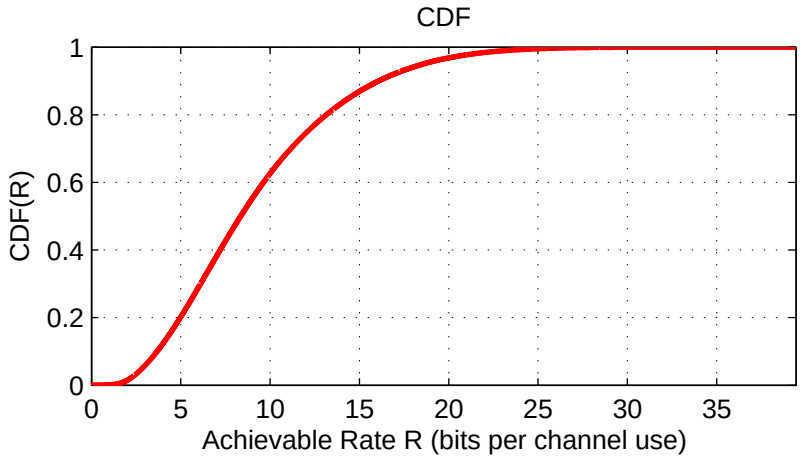

Figure 4.16: CDF of the topology in figure 4.10.

4.5 Limitations

The developed simulation tool is able to process and simulate quite arbitrary network setups. Nevertheless, there are limitations. They split up in network limitations and technical limitations.

4.5.1 Network Limitations

Network assumptions: This simulation tool assumes that each sector serves exactly one MS and transmits at full power. This distribution of MS is not very realistic. A more representational approach would be to have a random amount of MS per sector.

Cooperation schemes: Only one method performing cooperation has been implemented. For a more rigorous analysis of future cellular networks, more cooperation schemes need to be implemented. They can simply be added to the existing tool.

Frequency reuse: The user needs to assign frequencies manually to each BS. An automated distribution of frequencies is not implemented. What's more, one might have need to simulate dynamic frequency allocation according to the desired rate. Such an approach has not been implemented, though.

RS: The *decode and forward* approach for RS is only one of many possible RS configurations. However, other approaches are not implemented. Furthermore, it is not clear whether the used RS state approach is good. There might be more realistic approaches than turning RS on with a certain probability. For instance, simulating a MS in each sector individually and then deciding whether other RS are on or off might be more realistic.

4.5.2 Technical Limitations

Speed: Using this tool to run simulations with a reasonable high amount of repetitions per grid point is very time consuming. Most notably in a setup with cooperating sectors, the optimization process demands high computational resources and/or long simulation times. A remedy would be to use a compiled program, such as C/C++, for the simulation part. This would increase speed substantially. The implementation in another programming language, however, is arduous work and very time consuming. Parallel clustering can speed up simulation time as well even without using another programming language. This might lead, however, to another problem (see next point).

Licenses: Using parallel clustering does enhance simulation speed to a large extent. The drawback of this approach is the amount of Matlab licenses needed, as each running simulation requires a separate license. Similar to the first point, a compiled program, such as C/C++, performing the simulation part should, depending on the implementation, not require any additional licenses if run in parallel.

Cooperating sector borders: In section 4.2.3 about the functionality of cooperation, it was mentioned that sector borders are computed. Unfortunately, the algorithm performing this task is not very sophisticated. In fact, it works well for setups, where the cooperating sectors point more or less towards the geometric mean on the grid of the cooperating sectors. It is not clear, however, up to which deviation from such a setup this algorithm still produces usable sector borders. In the worst case, the borders need to be defined manually before starting a simulation.

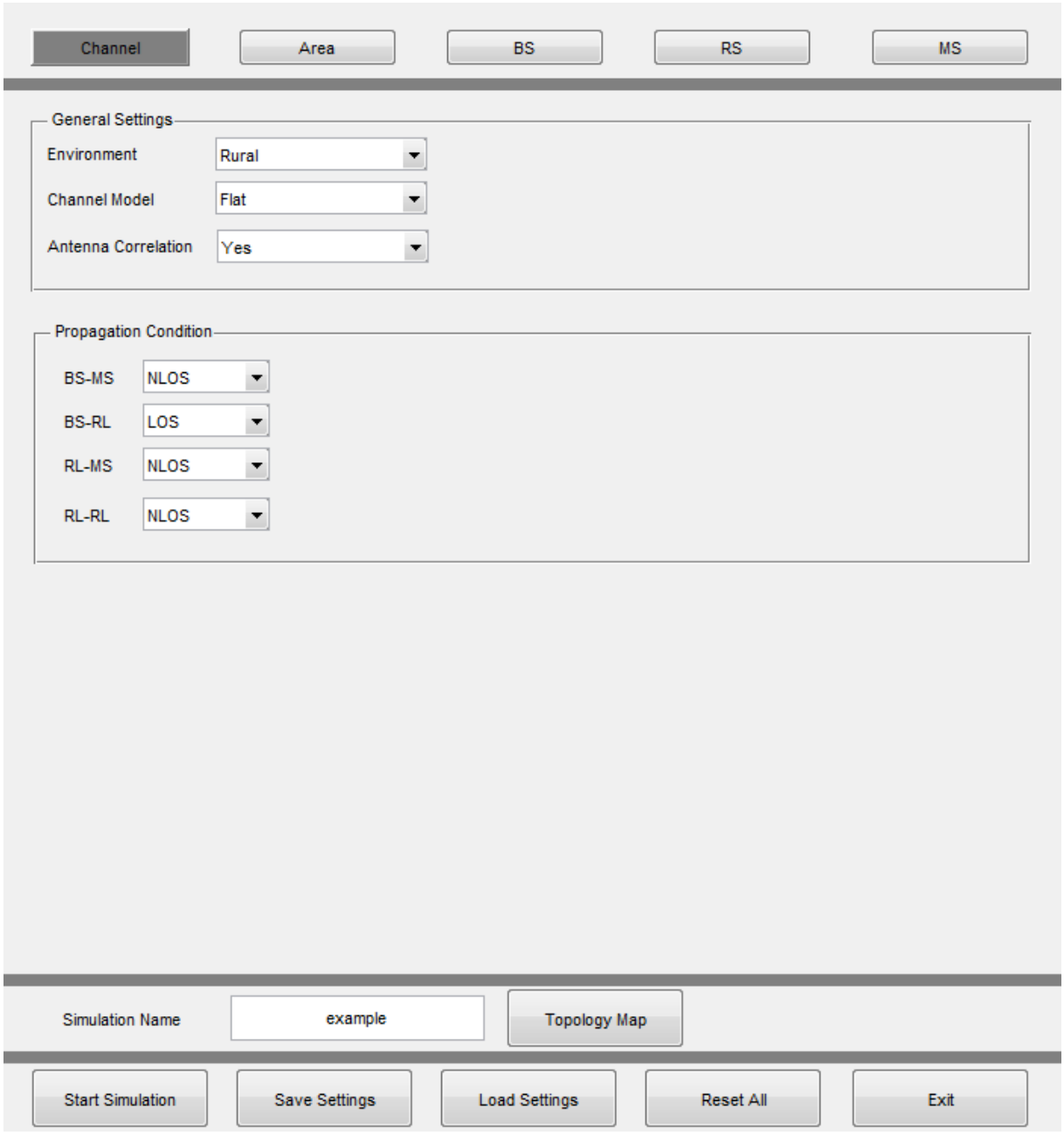

Figure 4.3: Channel tab of the preparation tool.

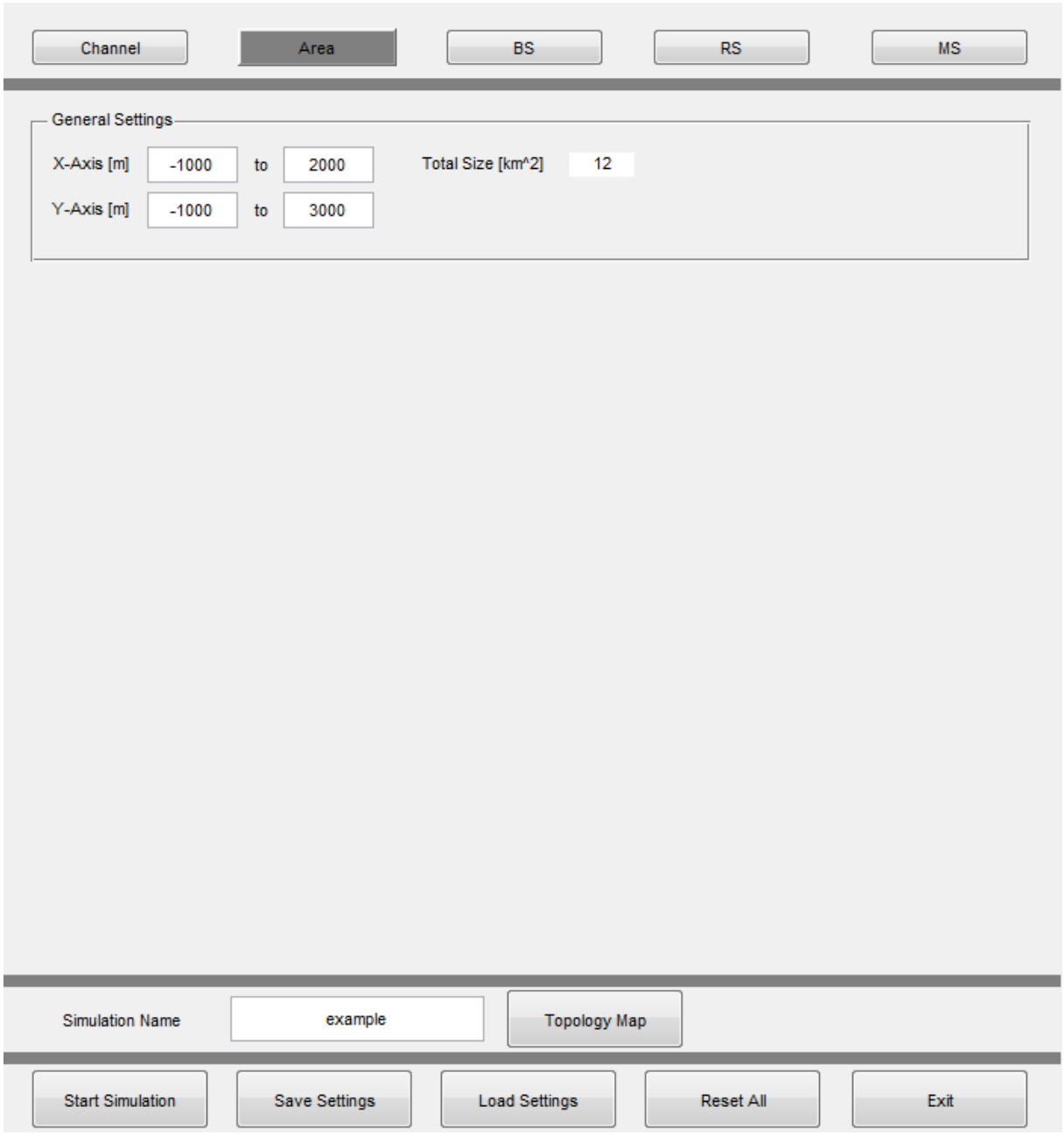

Figure 4.4: Area tab of the preparation tool.

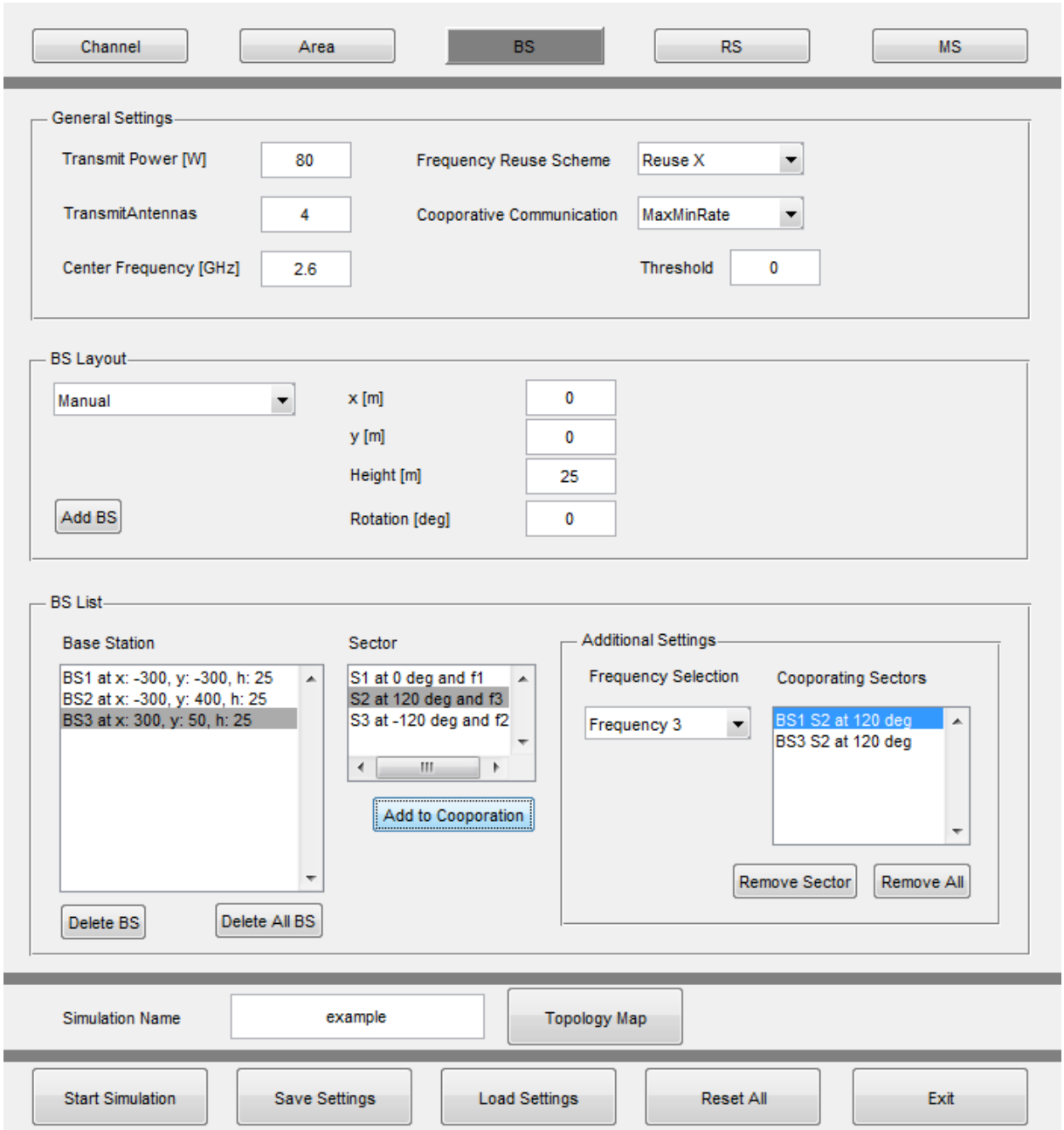

Figure 4.6: BS tab of the preparation tool.

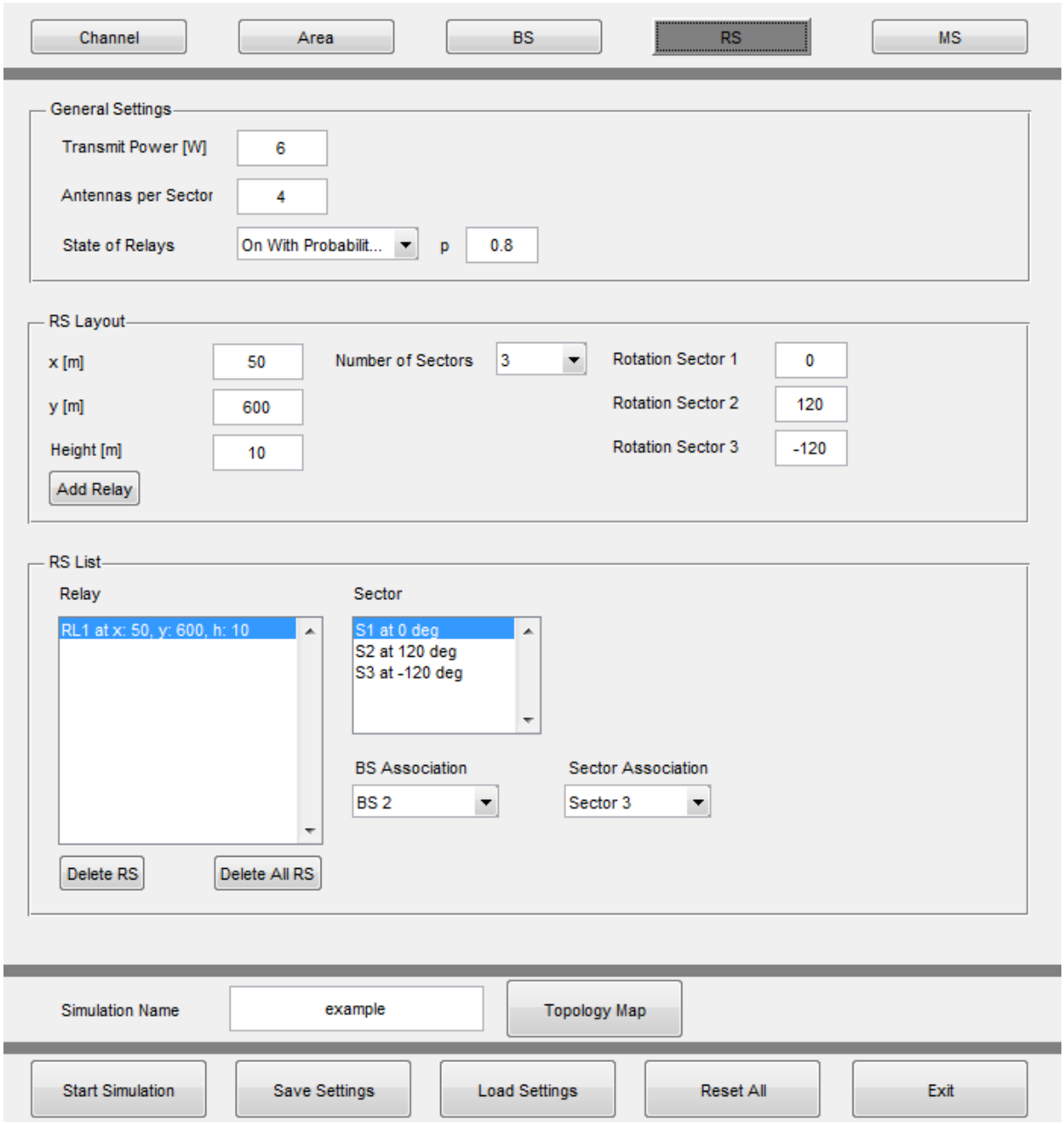

Figure 4.7: RS tab of the preparation tool.

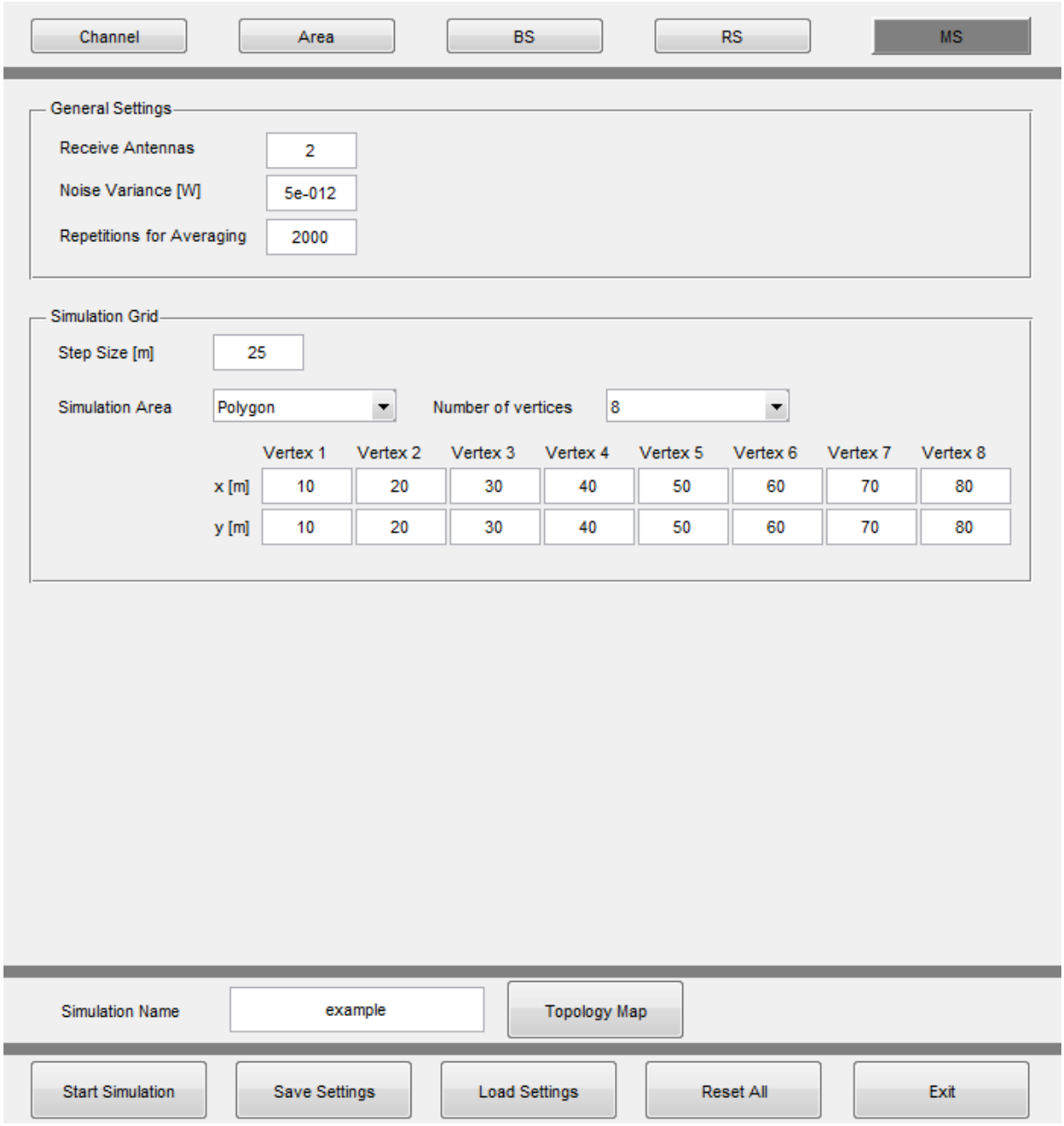

Figure 4.8: MS tab of the preparation tool.

Chapter 5

Simulations

In this chapter, the simulation tool described in the previous chapter is used to simulate a small selection of networks. The networks were chosen or designed such that a diverse amount of cellular network aspects are handled by the simulation tool. These aspects are frequency reuse, cooperation, and relaying. In section 5.1, the simulation results of a four BS network are presented. Cooperation as well as frequency reuse methods have been used for this network. A topology which cover a larger area has been analyzed in section 5.2, again with cooperation as well as frequency reuse methods. The network inspected in section 5.3 has the interesting feature, that due to cooperation, it uses less BS than a traditional cellular network might deploy. Lastly, a small selection of topologies including RS are presented in section 5.4. A few parameters are the same for all simulation rounds and are, therefore, listed here:

- The transmit power per BS sector is 80 Watts.
- The noise variance at the receiver is $5 \cdot 10^{-12}$ Watts.
- The center frequency is 2.6 GHz.
- The amount of transmit antennas at the BS is 4 and the amount of receive antennas at the MS is 2.
- All antenna arrays are correlated.
- The environment for the channel model is *rural*.
- All propagation conditions are *NLOS* with the exception of BS-RS links, these have *LOS*.

5.1 Simple Network

A simple setup with only four BS, each with three sectors, was used in this simulation. The BS were placed such that the four sectors in the middle point at each other. The other sectors don't point directly on an adjacent sector, see figure 5.1 for a detailed topology map. The network was simulated in four modified versions. Three different frequency reuse approaches and one with a cooperation area of the inner four sectors. For the cooperating scenario, the threshold for a minimum rate is et to 0 bits per channel use. In figure 5.2, the achievable rate for the four different modifications are depicted.

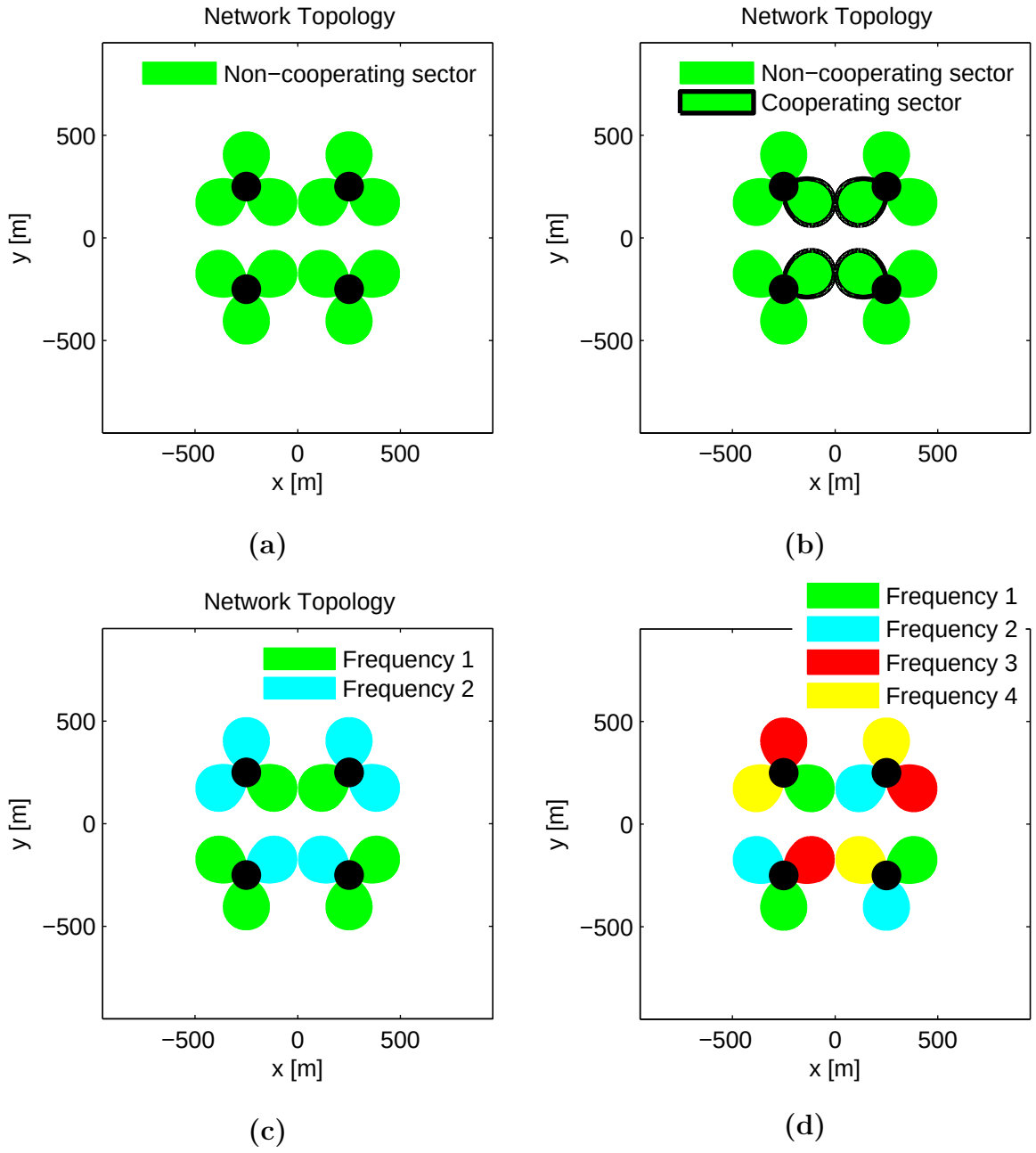

Figure 5.1: The four topologies used in this simulation: (a) each BS has the same frequency, (b) same as (a) but with cooperation, (c) two different frequency parts are divided among the BS, (d) four different frequency parts are divided among the BS.

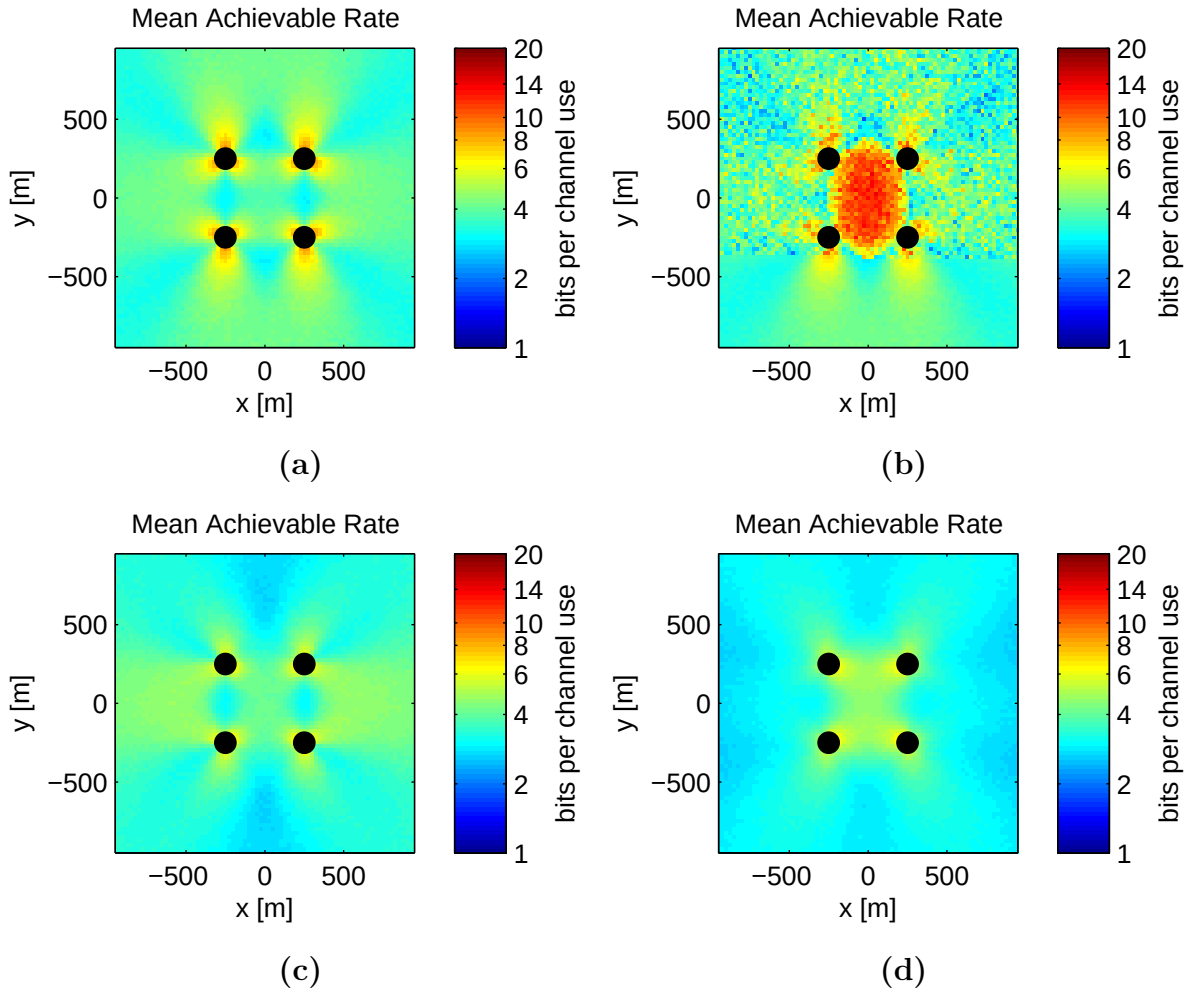

Figure 5.2: The mean achievable rate of the four modifications: (a) has the highest rate close to the BS as opposed to (c) and (d). (b) on the other hand has the highest rate of all in the middle due to cooperation.

5.2 Cooperation in a Conical Area

In this simulation, a more complex topology has been used, see figure 5.3. It is a modified version of the symmetric setup described in chapter 4 with a spacing d of 700 m. 22 BS serve an area of approximately 16 km^2. It is a setup with every second row of BS flipped horizontally.

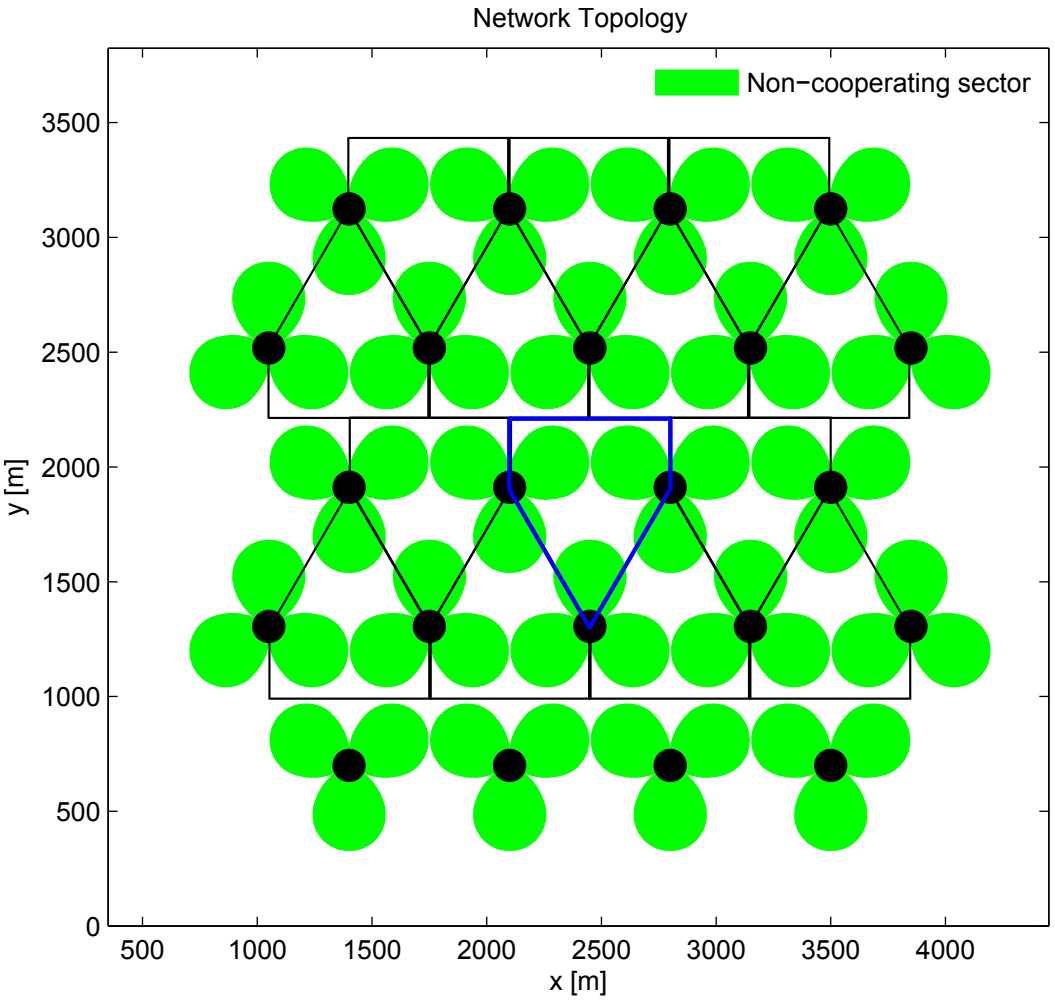

Figure 5.3: The network used in this simulation consisting of 22 BS. Due to symmetrical reasons, only the blue rimmed area has been simulated. This area can be used as a building block for the entire setup.

Due to the topology's symmetry, only a small portion of the whole area has been simulated, this is indicated in figure 5.3 by the blue revolved area in the middle. It is a conical shaped area. This simulated building block can be used to reconstruct the entire topology apart from edge effects.

In a first step, this building block has been simulated using one frequency portion only but once without cooperation and once with cooperation. The thus simulated area is depicted in figure 5.4. For the cooperating scenario, the threshold for a minimum rate is set to 0 bits per channel use.

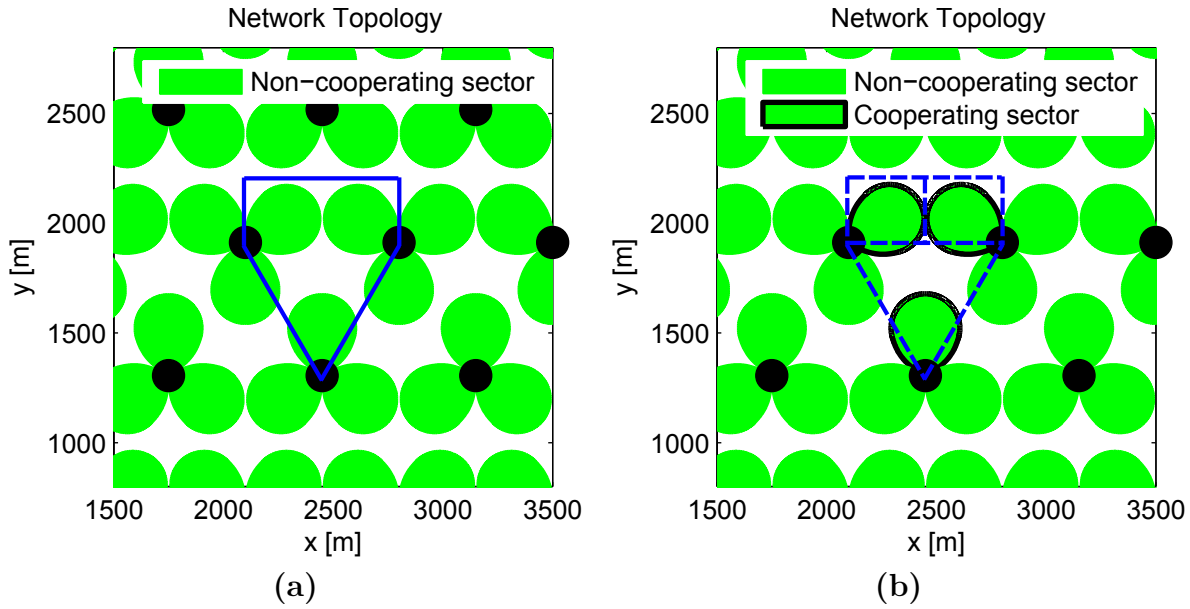

Figure 5.4: A close-up view of the conical simulation area. The simulation area is rimmed by the blue line. (a) is the non-cooperating setup, (b) is the cooperating setup with the blue dashed lines indicating the sector sizes used for the simulation.

After the termination of the simulation, the coverage has been computed using three different threshold values. The results of the non-cooperating setup and the cooperation setup are depicted in figure 5.5. In the non-cooperating network, close to the BS mean rates above 5 bits per channel use are achievable. However, in the middle of the simulation area, the mean rate does no exceed 2 bits per channel use. On the other hand, the cooperating network is able to fill this whole by distributing the mean rate more evenly over the simulation area.

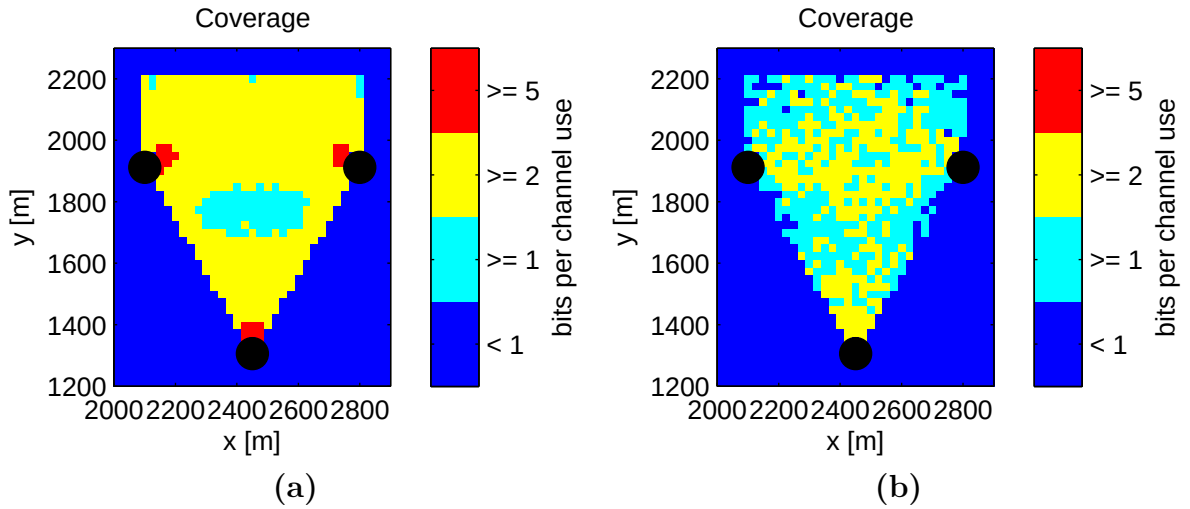

Figure 5.5: The coverage of the network depicted in figure 5.4. (a) is the non-cooperating network, (b) is the cooperating network.

In a second step, frequency reuse schemes were used in order to reduce interference from other BS. This was done for a non-cooperating setup as well as a cooperating setup. For the cooperating scenario, the threshold for a minimum rate is set to 0 bits per channel use. The corresponding topology extracts are depicted in figure 5.6. The resulting coverage plots are depicted in figure 5.7.

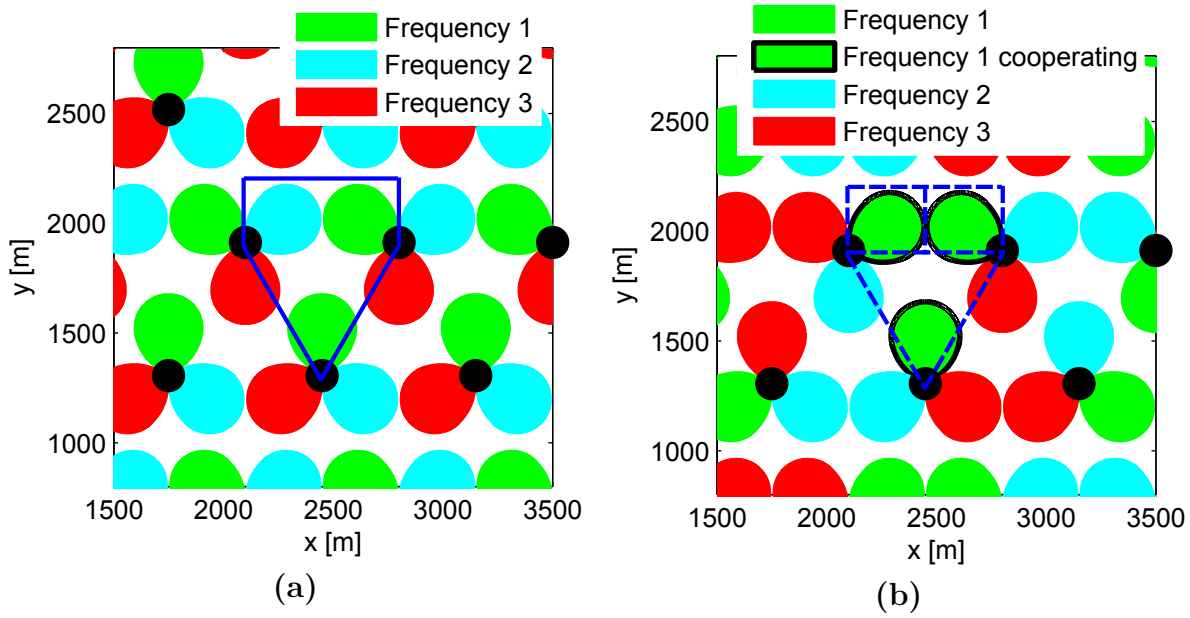

Figure 5.6: A close-up view of the topology. The simulation area is rimmed by the blue line. (a) is the non-cooperating setup, (b) is the cooperating setup with the blue dashed lines indicating the sector sizes used for the simulation.

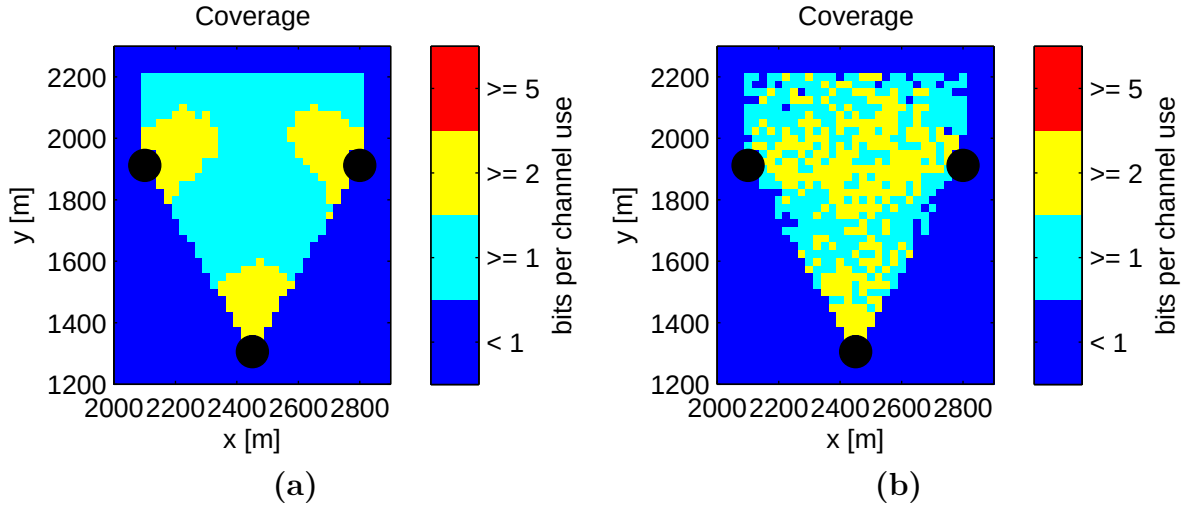

Figure 5.7: The coverage of the network depicted in figure 5.6. (a) is the non-cooperating network, (b) is the cooperating network.

In the non-cooperating scenario, the main lobes of the radiation pattern of the BS in

question become visible. Mean rates above 5 bits per channel use are not possible using a reuse 3 approach. The non-cooperating network is able to achieve rates above 2 bits per channel use close to the BS only. Similar to the reuse 1 network, the cooperating scenario distributes the rate more evenly over the simulation area. This is a clear improvement.

5.3 Cooperation in a Hexagonal Area

An interesting topology has been chosen for this simulation, see figure 5.3. It consists of 24 BS. It is a stripped version of the symmetric setup with spacing $d = 700$ m from chapter 4. Additionally to the stripping, individual BS were flipped horizontally. The result is a network in which always six sectors point on each other and serve a hexagonal area. Due to symmetrical reasons, only the blue revolved area in figure 5.3 has been simulated.

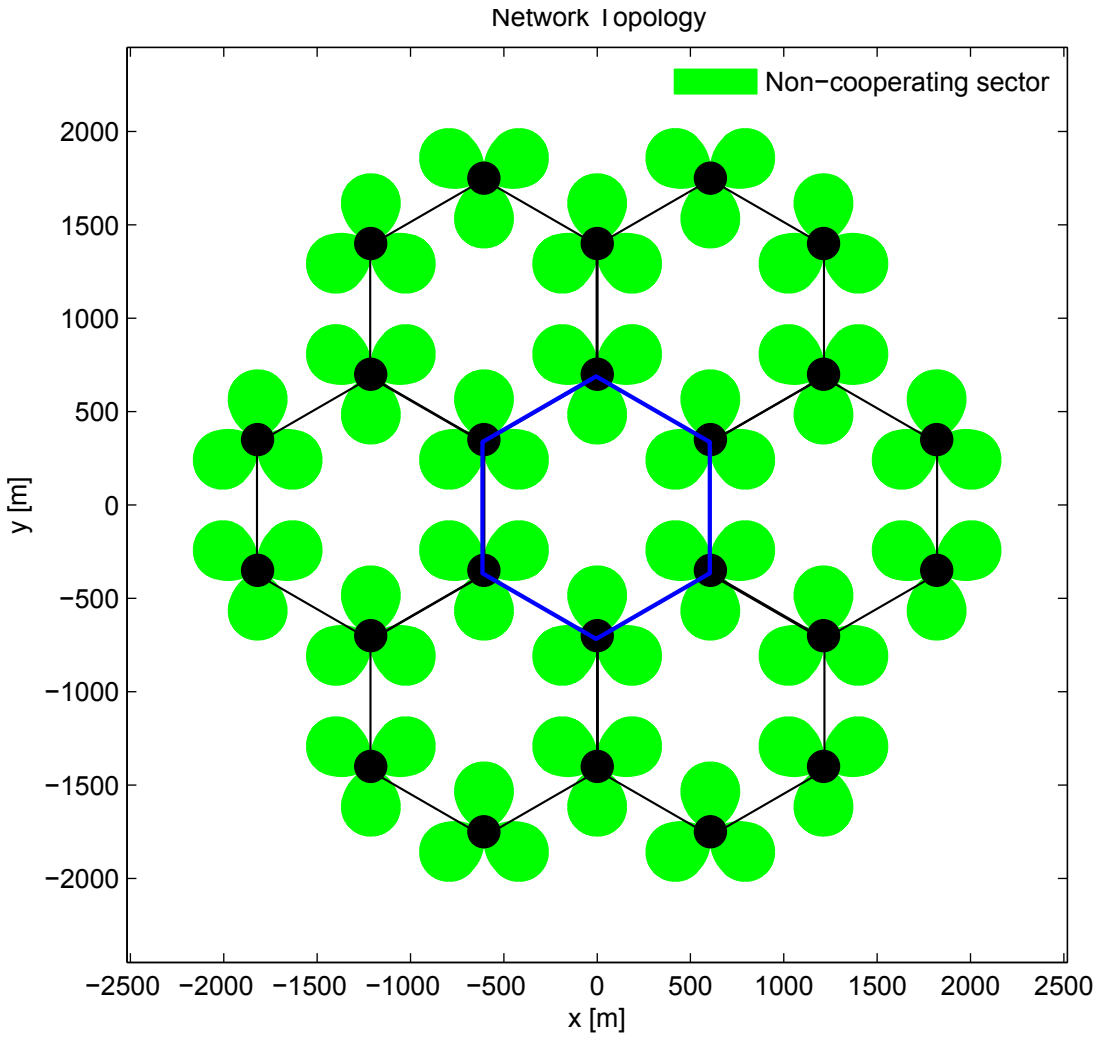

Figure 5.8: The network used in this simulation consisting of 24 BS. Due to symmetrical reasons, only the blue rimmed area has been simulated. This area can be used as a building block for the entire setup.

In a first step, the simulation was performed using one frequency only, once without cooperation and once with cooperation. For the cooperating scenario, the threshold for a minimum rate is set to 0 bits per channel use. The corresponding topology extracts are depicted in figure 5.9.

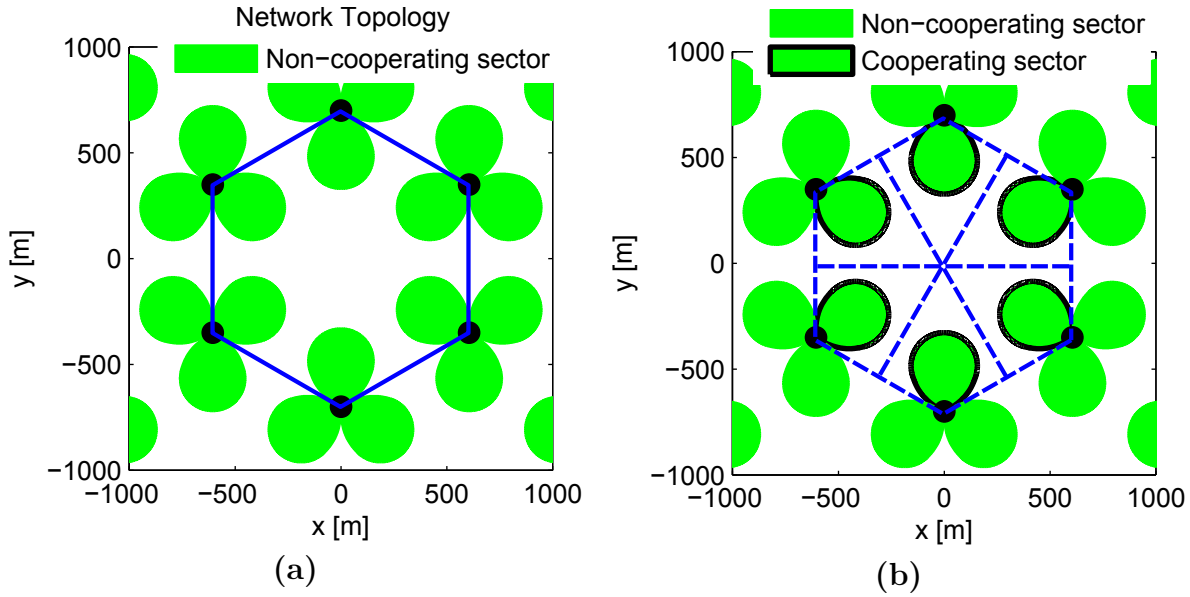

Figure 5.9: a close-up view of the topology. The simulation area is rimmed by the red line. (a) is the non-cooperating setup, (b) is the cooperating setup with the red dashed lines indicating the sector sizes used for the simulation.

After the execution of the simulation, the CDF of both the non-cooperating and the cooperating setup have been computed. The results are illustrated in figure 5.10. The cooperating network distributes the achievable rates better. This means that there are less high rates and less low rates. Most achievable rates accumulate in-between. An example: About 40% of all computed rates lie below 2.5 bits per channel use in the cooperating network. On the other hand, close to 70% of all computed rates lie below the same threshold in the non-cooperating network. In other words, even though higher rates are possible in the non-cooperating than in the cooperating network, there are more low rates in the non-cooperating than in the cooperating setup.

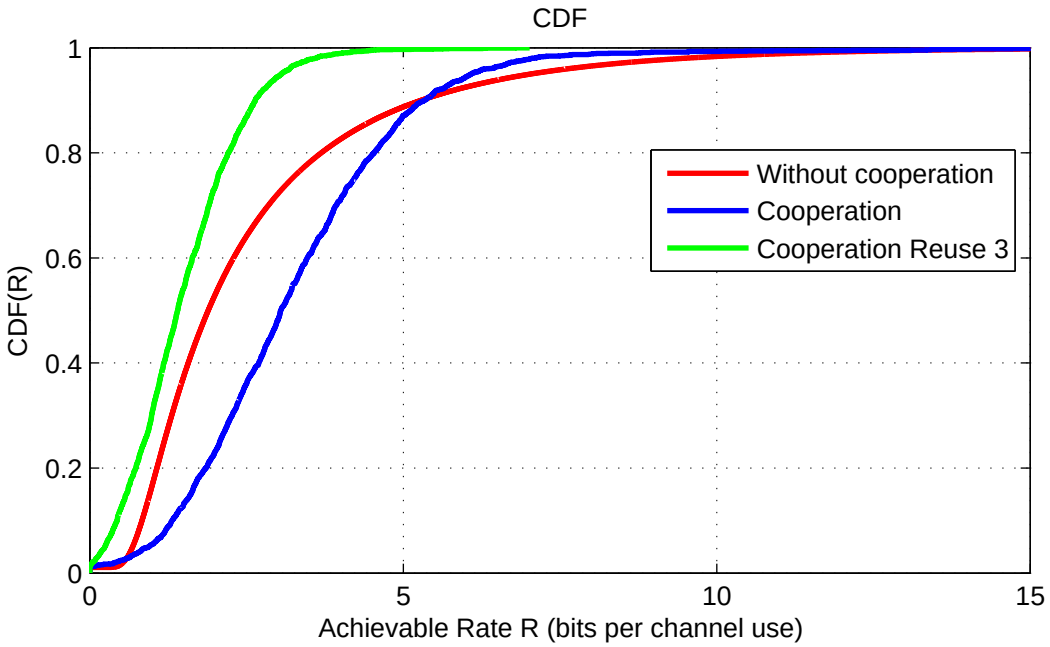

Figure 5.10: The CDF for the three setups simulated in this section.

In a second step, it a frequency reuse technique with three frequencies together with cooperation was applied. Each hexagon of six cooperating sectors has a different frequency than any of the six adjacent hexagons. This is depicted in figure 5.11. In such a network, the interference is reduced to some extent. The same area as for the cooperating case in figure 5.9 (b) was used for the simulation. The rate threshold was again set to 0 bits per channel use. The resulting CDF is depicted in figure 5.10. This network performs clearly worse than the cooperating setup with only one frequency. This can be based on the fact that the interference from adjacent hexagons is not so high as most sectors in the neighboring polygons do not point directly to the hexagon in question.

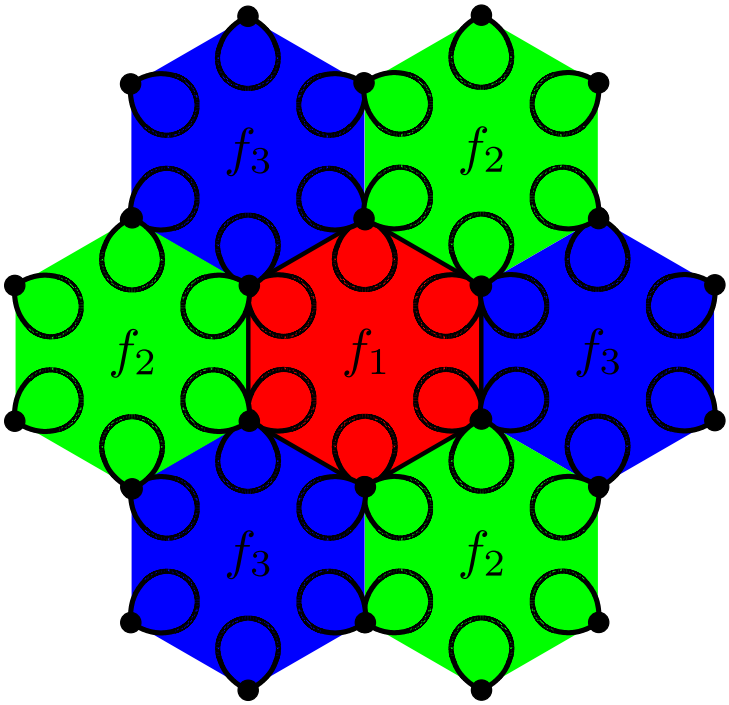

Figure 5.11: The distribution of the three frequencies f_1, f_2, and f_3 over the hexagonal setup with cooperation. The area pertaining to frequency f_1 is the simulation area.

5.4 Relaying

In a last simulation round a few networks were analyzed using RS. Figure 5.12 shows four different setups. The first one is a reference and, therefore, contains no RS. The second, third, and forth setup have the same BS as the first but additionally one RS at different locations, angles, or with different numbers of sectors. In all setups, the RS is associated with the BS sector at 90 degrees clockwise off the y-axis. Each RS sector transmits with a power of 6 Watts. It uses a correlated antenna array of four antennas.

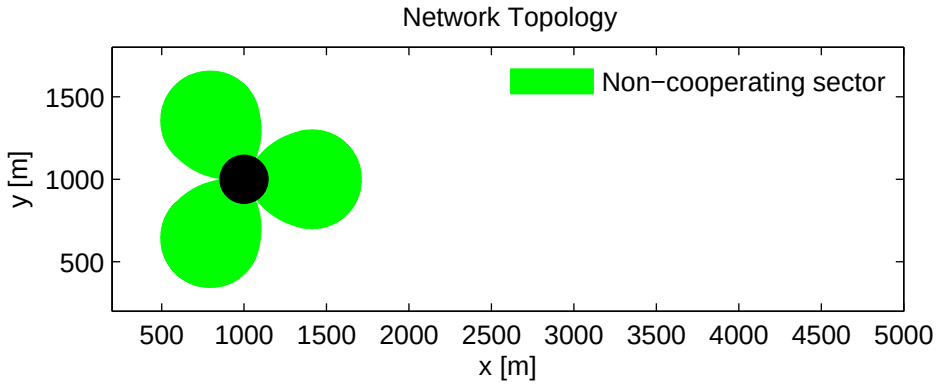

(a)

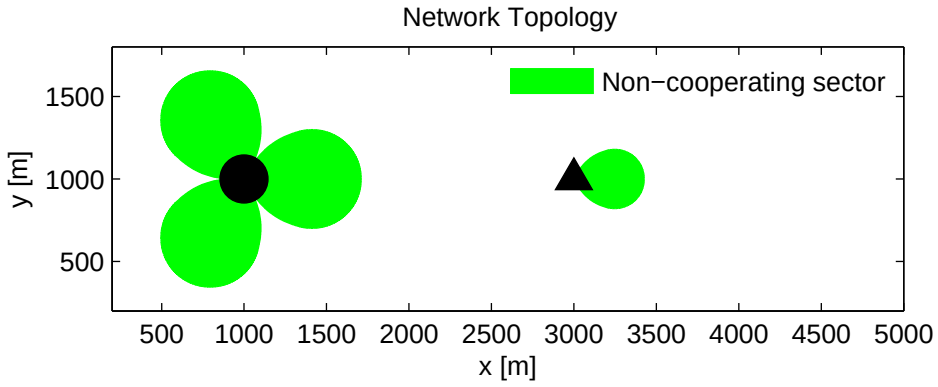

(b)

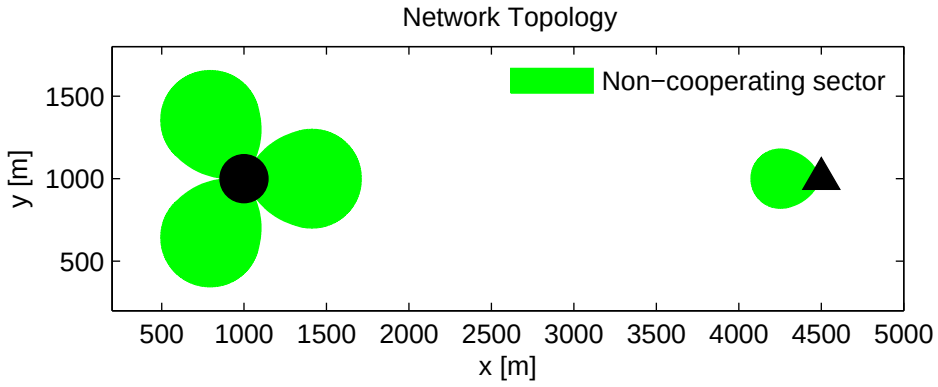

(c)

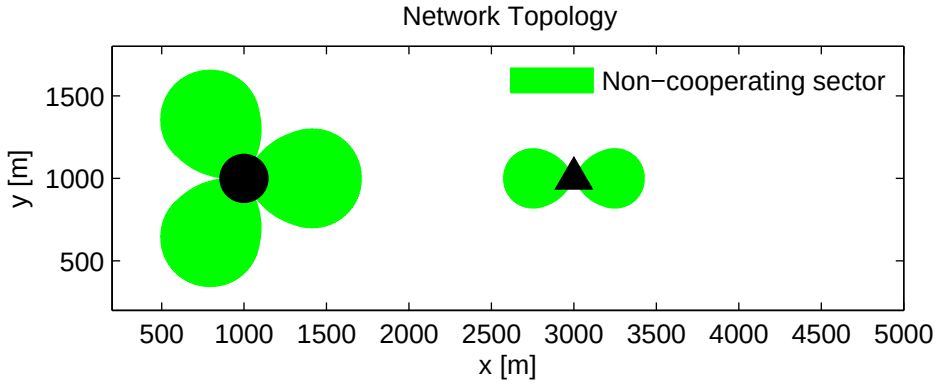

(d)

Figure 5.12: Four different setups with RS: (a) is a reference setup and has no RS. (b) uses one RS pointing away from the BS. (c) uses one RS pointing towards the BS. (d) uses one RS with two sectors, one pointing towards and one away from the BS.

The simulation results were processed by computing the outage rate. To this end, the 5% percentile was calculated. The resulting plots are depicted in figure 5.13. Very close to the RS the outage is improved. This is due to the diversity available: the direct rate from BS to MS or the link via RS. Further away from the RS the outage seems to be the same is if there was no RS. This is due to the relatively low transmit power of the RS of 6 Watts as opposed to 80 Watts of the BS. This improvement can be understood more clearly by viewing the cell size plots in figure 5.14. Close to the RS, the test MS connects more likely to the RS because it achieves a higher rate via RS than directly from the BS.

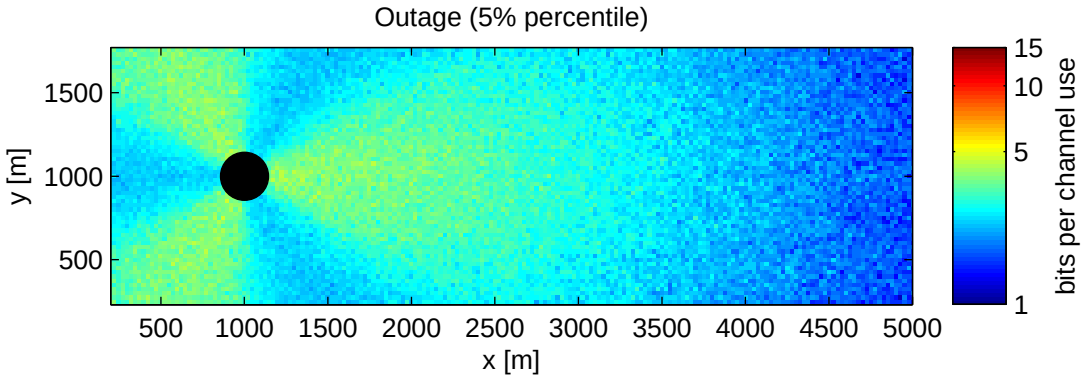

(a)

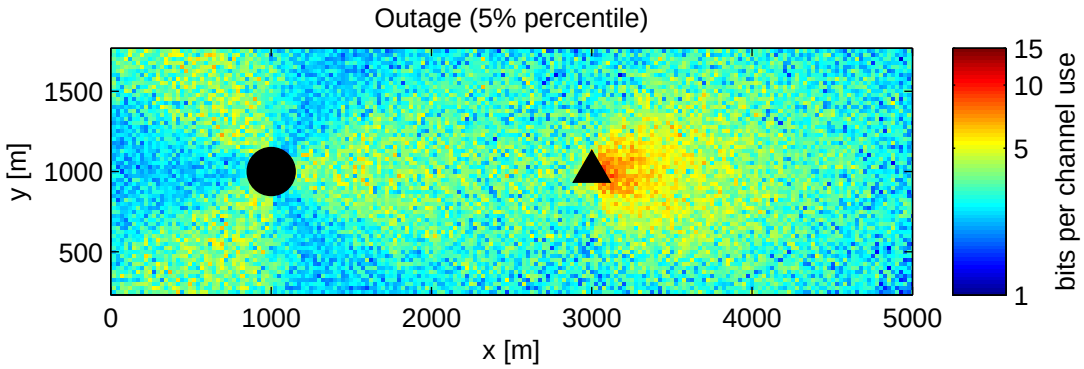

(b)

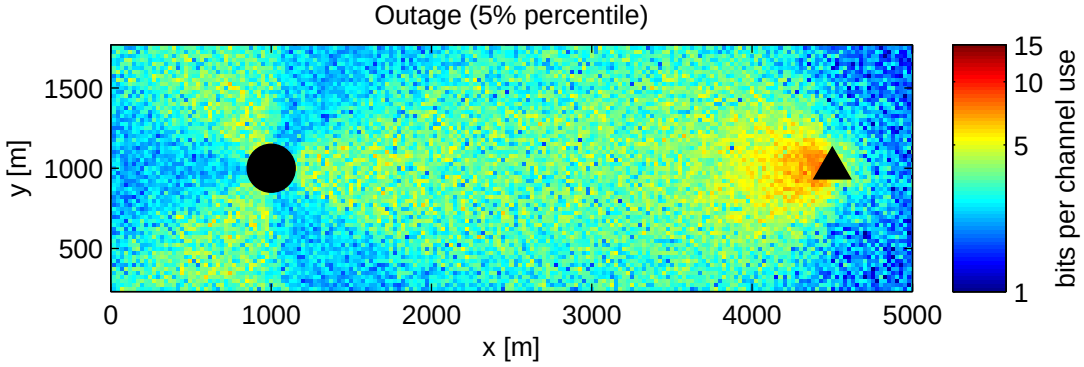

(c)

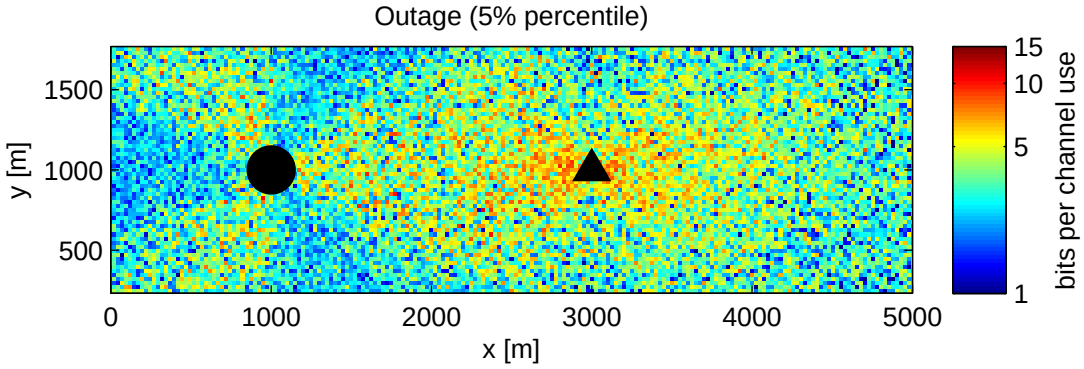

(d)

Figure 5.13: Outage (5% percentile) of the four simulated setups. The presence of RS clearly improves the outage close to the RS.

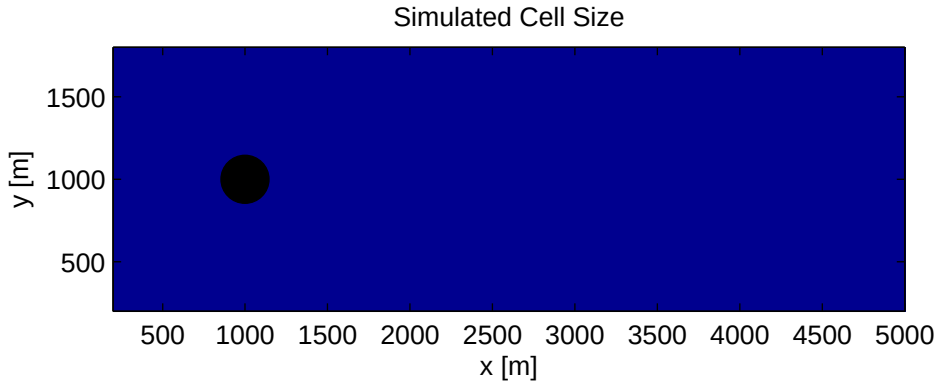

(a)

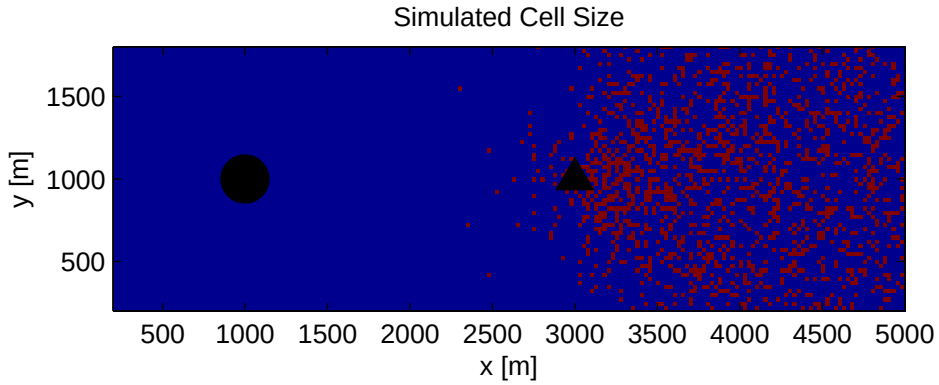

(b)

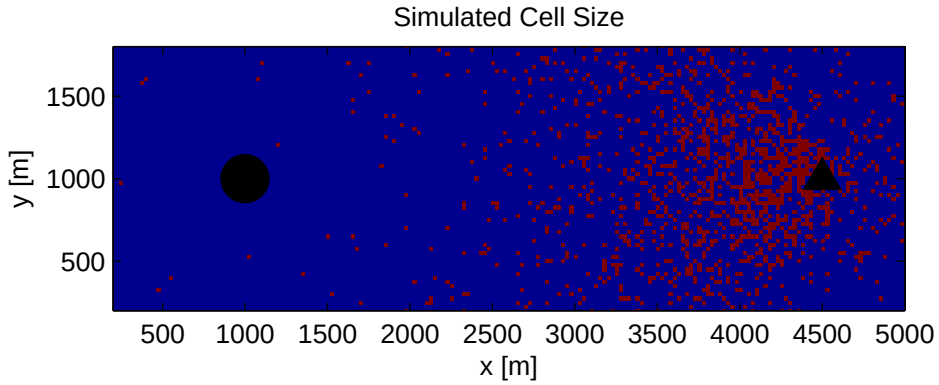

(c)

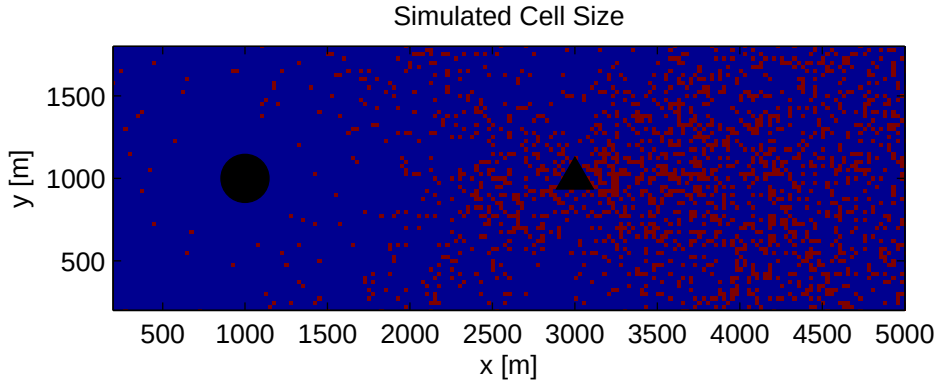

(d)

Figure 5.14: Cell size of the four setups.

Chapter 6

Conclusions

6.1 Conclusions

In this project, a generic simulation tool has been designed and implemented. The tool is modularly built and can be enhanced easily. There are a few features, however, which are in need of improvement. The algorithm used for the computation of sector borders in a cooperating setup does not produce satisfactory results for an arbitrary setup. Furthermore, the execution of the simulation can take a tremendous amount of time. In addition, only one network model with one MS per BS has been implemented.

The simulation tool has been used to successfully simulate a small selection of cellular networks. They were subsequently analyzed using the same simulation program. The results show, that a cooperation scheme using block diagonalization and an optimization algorithm, which assigns equal rate to all MS, improves the distribution of achievable rates. Furthermore, it has been shown that RS have the capability to enhance coverage and to improve the outage rate (5% percentile) of cellular networks.

6.2 Outlook

The simulation tool can be used as a basis of current and future simulation projects as well as in research activities. It can be improved and enhanced without excessive work and programming time. In particular, more options for the network model i.e. a random amount of MS per sector, or other cooperating techniques would be welcome. More channel models and more advanced RS techniques can be implemented and included in this tool.

A few of the networks simulated in chapter 5 could be interesting research topics for the future. In particular the hexagonal setup of section 5.3, where six BS cooperate,

is interesting, as traditional setups would use more BS in the same area. In addition, networks with RS are able to improve the outage as the RS introduces additional diversity to the network. Other RS techniques as a simple *decode and forward* approach are surely interesting for future research activities.

Bibliography

[1] A. Lapidoth. *A Foundation in Digital Communication*. Cambridge University Press, New York, 2009.

[2] D. Tse and P. Viswanath. *Fundamentals of Wireless Communication*. Cambridge University Press, New York, 2005.

[3] E. Telatar. Capacity of Multi-Antenna Gaussian Channels. *European Transactions on Telecommunications*, 10:585–595, 1999.

[4] H. Bölcskei. *Fundamentals of Wireless Communications*. Lecture Notes ETH Zurich, Feb 2008.

[5] J. Löfberg. YALMIP: A Toolbox for Modeling and Optimization in Matlab. In *Proceedings of the CACSD Conference*, Taipei, Taiwan, 2004.

[6] K.C. Toh, M.J. Todd, and R.H. Tutuncu. SDPT3 - A Matlab software package for semidefinite programming. *Optimization Methods and Software*, 11:545–581, 1999.

[7] M. Kuhn. QoS in Wireless Networks. Lecture at ETH Zurich, 2010.

[8] P. Kyösti. *WINNER II channel models*. WINNER, Tech. Rep. IST-4-027756 WINNER II D1.1.2 V1.2 Part I Channel Models, 2007.

[9] T. M. Cover and J. A. Thomas. *Elements of Information Theory*. Wiley Inter-science, 1st ed. edition.

[10] YALMIP Wiki. Logdet, Jan 2011. `http://users.isy.liu.se/johanl/yalmip/pmwiki.php?n=Commands.logdet`.